Granular Composite with Addressable and Tunable Stiffness

Ahmed A. Elashwah

Dissertation submitted to the Faculty of the
Virginia Polytechnic Institute and State University
in partial fulfillment of the requirements for the degree of

Master of Science
in
Mechanical Engineering

Michael D. Bartlett, Chair
Robert L. West
Ling Li

July 08, 2024
Blacksburg, Virginia

Keywords: Granular Jamming, Granular composite, Stiffness, Pneumatics

Granular Composite with Addressable and Tunable Stiffness

Ahmed A. Elashwah

(ABSTRACT)

An integral part in the field of soft robotics is the ability to tune material stiffness. This adaptability is inspired from the natural ability of organisms to alter their stiffness to perform various tasks. The most common approach to mimic this ability is through granular jamming, where a granular material switches between fluid and solid-like states based on density alterations caused by vacuum pressure. In this thesis, a cuboid composite material is introduced, containing internal cylindrical chambers arranged in distinct matrix configurations (2x2, 3x3, and 4x4). A custom-designed pneumatic system enables precise control over this transition, allowing for selective modulation of stiffness across different regions of the material by applying differing pressures to specific regions of the composite material. This approach not only allows for rapid changes in stiffness, but enables stiffness to be adjusted uniformly throughout the material or localized to specific areas. This approach also allows for predictive modeling of granular composites to better understand its mechanical response under differential pressures.

Granular Composite with Addressable and Tunable Stiffness

Ahmed A. Elashwah

(GENERAL AUDIENCE ABSTRACT)

Soft robotics is a field that mimics the flexibility of living organisms such as octopi, geckos, etc., to create machines that can adapt to various tasks and environments. One of the unique features of these robots is their ability to change how stiff or soft they are, much like an octopus can alter the rigidity of its tentacles when gripping an object. A method called granular jamming is at the heart of this technology. It involves using materials made up of tiny particles, like coffee grounds or sand, that can switch between flowing freely like a liquid and locking together like a solid. This switch is controlled by changing the space between the particles, usually by sucking out air to pack them tightly. The research in this thesis introduces a special type of material designed as a rubber-like cube containing multiple small cylindrical compartments arranged in different patterns, such as 2x2 or 4x4 grids. Each compartment is filled with these unique particle-based materials, in this particular instance, the material is coffee grounds. We use a specially designed air pressure system to selectively adjust the air pressure in these compartments, making the material stiffer or softer as needed. This allows us to control the stiffness with great precision, either uniformly across the whole block or in specific areas. The experiments conducted in this thesis show a clear pattern: the more air pressure is decreased (making it more negative), the stiffer the material becomes. This finding confirms that granular jamming is a promising strategy for rapidly and precisely controlling material stiffness for future soft robotic applications.

Dedication

To my father, mother, and brother. This wouldn't have been possible without you.

Acknowledgments

First and foremost, I owe a tremendous thank you to my advisor, Professor Michael Bartlett. Professor Bartlett's relentless support, encouragement, and expert guidance didn't just steer the course of this thesis; they made every challenging moment manageable and every achievement more meaningful. His passion for precision and commitment to excellence not only enriched my research experience but also set a high bar that inspired me daily. I am also immensely grateful to Professor West and Professor Li. Professor West's keen insights and strategic thinking pushed me consider other perspectives that have not occurred to me prior, and have only helped to strengthen my thesis. I would also like to thank Professor Li for his encouragement and kindness throughout this work. Their kindness and understanding throughout this process is something that I will always appreciate, and am eternally thankful for. I would also like to thank my undergraduate thesis advisor, Professor Ramadi, for allowing me to conduct research in his lab and sharing with me his experience in research. I would also like to thank Professor Daqaq, my undergraduate advisor, for his help and support in inspiring me to pursue my graduate studies at Virginia Tech. He spoke highly of Virginia Tech's research program and his graduate school experience there. This experience inspired me to apply to Virginia Tech, where I met amazing faculty and students. I would like to thank all members of the Soft Material and Structures research group for creating a welcoming and supportive environment. I thank Ohnyoung for first introducing me to the lab and showing me the ropes. I thank Wuzhou, who assistance with ordering much needed supplies for my research has proven invaluable. I thank Brittan and Daniel, whose help with fixing the 3D printer helped my work run smoothly. I thank Ravi and John, whose assistance has allowed me to grow and develop as a researcher. I also thank the remaining members

of the Bartlett Lab group. You all have provided me with fresh insights, wisdom, support, encouragement, and more help than I can put into words. I wish you all the best in your academic and research journeys. To my family—words cannot fully capture my appreciation. I want to thank my parents, Rania and Adham, whose boundless love and unwavering support have been the foundation of my journey. The countless sacrifices you've made are deeply acknowledged, and your belief in my potential has been a never-ending source of strength. To my brother, Asser, thank you for being there with your humor and steadfast encouragement. Your ability to turn even the most stressful of circumstances into humorous moments has helped me get through this rigorous academic pursuit. Without your love, support, and encouragement, I would not be where I am today. Thank you all very much.

Contents

List of Figures

List of Tables

Chapter 1

Introduction

The development of materials with tunable strength and stiffness is not just key to material science, it is key to mechanical engineering. As mechanical engineers, the properties of the materials used in automobiles, planes, robotics, and aerospace applications are essential. Even though material properties are determined by their atomic and molecular configurations and microstructure, their properties can be controlled depending on its geometry, life cycle, or external stimuli (Ex. electrical, thermal, etc.).

A material with customizable, tunable stiffness has been the focus of material scientists and engineers for years. Advancements in regards to a material with tunable stiffness focused on a material with custom mechanical properties, thermal properties, and microstructures for use in specific applications, but there has been no research into a material that is capable of changing its stiffness in a controllable manner. An approach to control the stiffness of materials is to jam it, changing it from being in a soft, fluid-like state to a solid-like state with a higher yield stress [17]. This process occurs when the viscosity of various materials increases alongside particle density.

In this thesis, I have adopted the phenomenon of granular jamming for addressable and tunable stiffness utilizing pneumatics. Granular jamming is a process in which granular materials increase their packing density when compacted together in a small, enclosed space, and has been used for gripping applications [3] [36], switchable morphing aerospace structures [13], shock absorbers [31], haptics [70], selectively stiffening garments [40], and switchable

adhesives [27].

1.1 Granular Materials and Tunable Stiffness

Granular materials, foams, and colloids are commonly used when investigating granular jamming applications. Examples of granular materials are sand, coffee grounds, glass beads, metallic beads, or any material with grain-like properties. These materials have a low packing density that increases drastically when the grains are subjected to a load (usually in the form of vacuum pressure) that creates "force chains" along their compressional axis [16]. In this jammed state, the granular materials have switched from being in a fluid-like to a solid-like state. Tunable stiffness is the ability to manipulate the stiffness of a material by controlling its properties. Magnetorheological elastomers can change their stiffness via a magentic field response [7], liquid metal composites via thermodynamic relaxation [18], and other materials utilize light, solvents, vacuum, and electric stimuli to produce a change in material properties [13, 18].

The aim of this work is the development of a material with addressable and tunable stiffness and to develop an understanding of how this material behaves through characterizations, shape distributions, and deformation. This thesis comprises four sections, an introduction, a literature review, an experimental section, and a final section that discusses the conclusions reached in this work. Throughout this work, applications of soft robotics and granular jamming are discussed (Chapter 2). The concepts behind these applications are used as the foundation behind various soft robotics applications, ranging from aerospace structures to haptics and switchable adhesives. Throughout this work, various designs for the granular composite material were developed and tested to observe the effect of granular distribution on stiffness (Chapter 3). As discussed, pneumatics allow for switchable granular jamming

to occur inside of the composite material without changing the chemical compositions.

1.2 Organization of Thesis

In this thesis, tunable stiffness is achieved using an elastic material (silicone rubber) and granular material (coffee grounds) to develop a composite modulated by granular jamming that is adjusted with customized pneumatics.

Chapter 2 introduces the background literature of the approach, where the primary concepts of granular jamming and stiffness tuning techniques are explained in further depth.

Chapter 3 describes our approach, where we apply the granular jamming concept to develop a composite material with controllable and adjustable stiffness. Three different configurations of the composite material are developed to explore how granular distribution can affect overall stiffness. This is achieved by fabricating a custom pneumatic system that is capable of adjusting the negative pressure inside of a predefined region of the sample.

Chapter 4 summarizes all thesis work and discusses the contribution and future applications of this research.

Chapter 2

Literature Review

2.1 Introduction

Developments of smart material composites rely on stimuli such as but not limited to electricity, heat, magnetic fields, and pressure to induce a change in material properties [18]. Advancements have focused on composites that respond to a specific stimulus, which results in a property change [18]. Soft materials can be programmed into desired shapes with desired properties that are utilized in soft and bio-inspired robotics. In fact, the ability to switch a material's state from flexible to rigid and vice versa has numerous applications in robotics [14, 20, 45, 49, 60, 68]. Additionally, composite materials with variable stiffness have applications in deployable structures, damping, and aerostructures [13, 74]. Particle jamming (sometimes referred to as granular jamming) under reduced pressure can be used to transition a material from a fluid-like state to a rigid solid state [30]. A common approach for controlling jamming and stiffness of granular media is the development of pneumatically activated systems [28, 30]. This review will discuss the concept of granular jamming, modeling particle jamming, and its applications.

2.2 Granular Materials

Granular materials are a class of materials that undergo a transition from mechanically unstable to mechanically stable states as key systems parameters change [9]. Simply put, granular materials are large combinations of discrete particles, such as sand, coffee grounds, rice, etc. in contact and surrounding voids [2, 32, 33]. Their behavior is determined not by their arrangement, but by the types of interactions among them [32]. In general the spaces between the particles are filled with an interstitial fluid, usually air [15]. However, it will be assumed herein that the particles are large and heavy in the sense that they are immune to effects of the interstitial fluid [15].

2.3 Physics of Granular Jamming

Granular jamming is the result of a change in a key system parameter that alters the density of granular materials, preventing particle motion [9]. In order to induce any motion in granular materials, vibrations are necessary [9]. As the intensity of vibrations is lowered, the material transitions from a fluid to a solid with yield stress [9]. This not only occurs with grains but with other soft materials like gels [70]. In controlled locomotion, actuation, and stiffness tuning applications, having parts that are mechanically re-configurable is critical [18]. In most jamming designs, the object consists of a flexible membrane/shell filled with a granular material [28, 70] as shown in Fig. 2.1.

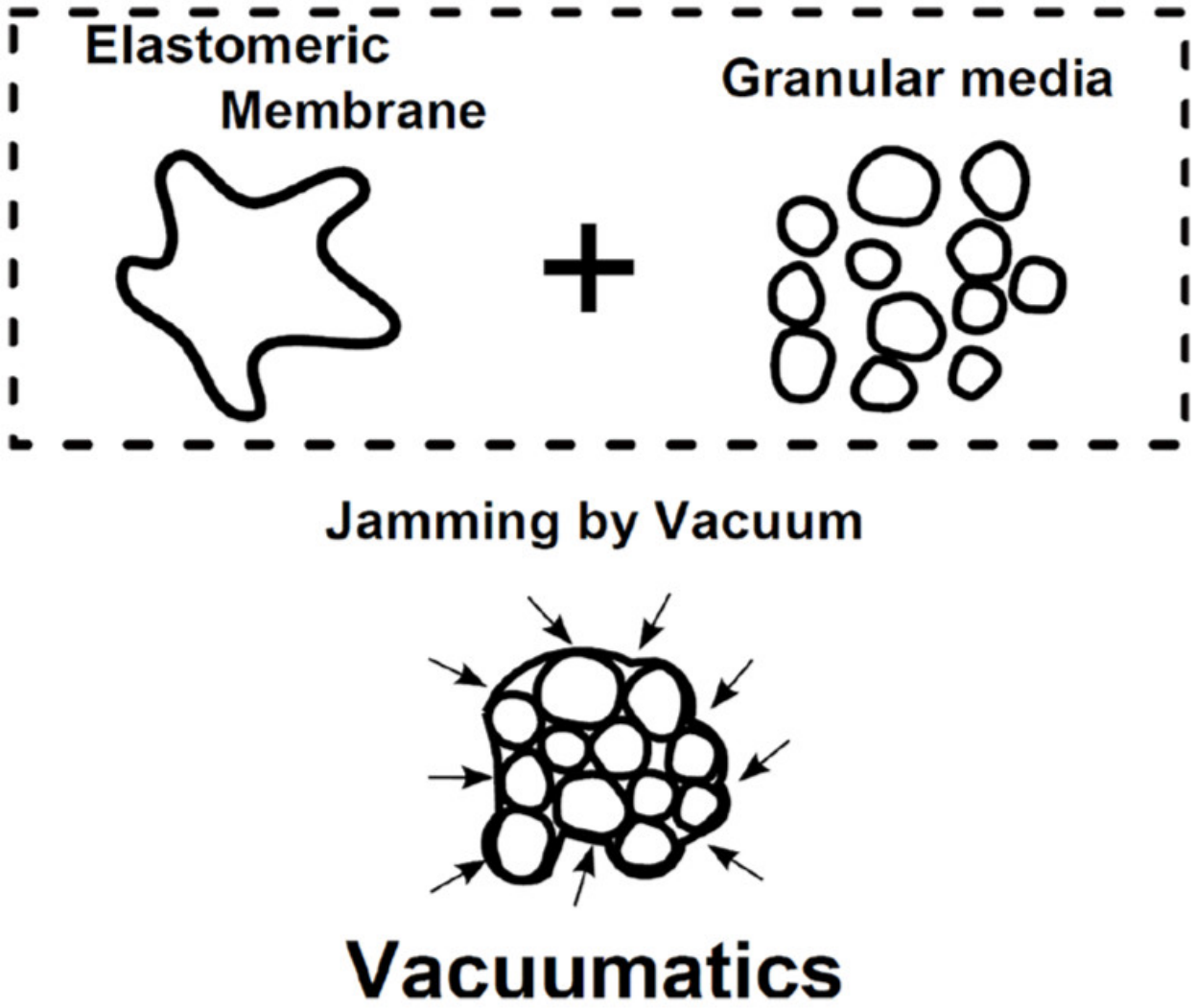

Figure 2.1: **Granular Jamming by Vacuum [13]. Reused with permission.**

When that composite material (flexible membrane/shell filled with a granular material) is in its natural state, it is soft, elastic, and malleable. When it is in a jamming state (caused by a vacuum being applied to remove air) it is a firm, hard object. Loose, unjammed grains behave as fluids, while rigid, jammed grains behave as solids [26]. When a vacuum is applied to the container of the granular media, the internal volume is reduced, whereas the external force from atmospheric pressure forces the granular particles together [13, 28]. It has been proposed that if the direction of the applied stress in a jammed material changes by even a

small amount, the jam will break up [46]. An example of this is a pile of sand: it appears solid, sustains its shape despite gravity, but if the pile experiences vibration, the sand grains shift and it no longer appears to be a solid [46]. Jamming occurs because the particles form "force chains" along the compressional direction, or in this case, the direction the air is being removed in [16]. Jamming is used in soft robotics as considerable stiffness variation can be achieved with minimal volume variation.

There are many possible variations of jamming structures that are easily adapted for different soft robotics applications, e.g., for gripping, locomotion, as well as shock resistance as a limb, end effector (the device at the end of a robotic arm designed to interact with the environment) and body (main structure of the soft robot) [26].

2.4 Modeling Particle Jamming

In robotic applications, a particle jamming part can act as a cheaper alternative for a robotic gripper where the robot presses the mass of the unjammed material around an object and then jamming it to create a rigid grip [68]. In medical applications, thin particle jamming tubes have been tested for their applicability as an endoscope with controllable rigidity [68]. The physics behind particle jamming are as follows. Starting with a simple model of a force chain (linear string of rigid particles in point contact) that can support loads along its own axis, therefore the forces along the contact line must be collinear [16]. Now picture this: instead of a jammed gel-like material, visualize an assembly of force chains in an incompressible solvent [16]. Do not assume any collisions between the force chains or deflections [16]. To model the pressure tensor with no body forces acting ($p_{ij} = -\sigma_{ij}$) is written as follows:

$$p_{ij} = P\delta_{ij} + \Lambda n_i n_j \tag{2.1}$$

Where P is isotropic fluid pressure, n is the direction vector (n_i and n_j respectively), and Λ (>0) is the compressive stress carried by the force chains [16]. As long as the applied force is along the n vector, loads can be applied reversibly via an elastic mechanism as seen in Fig. 2.2.

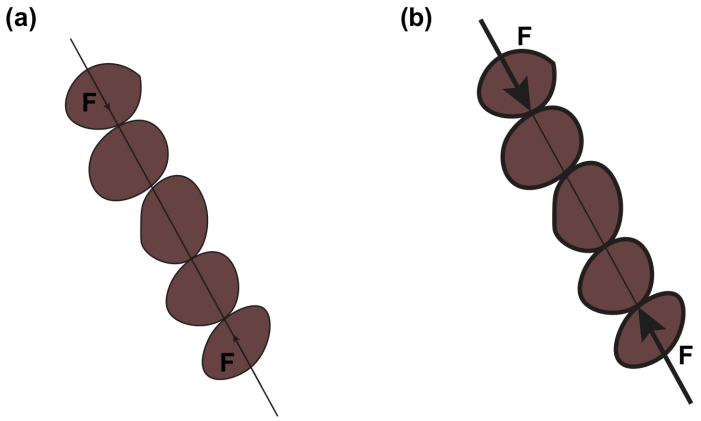

Figure 2.2: **Granular Chain Compression.** **(a)** A force chain of particles (shape is irrelevant) can support only longitudinal compression. (Directly acting body forces are neglected). **(b)** Finite deformability allows small transverse loads [16].

A disadvantage of the force chains is that the material is not an elastic body, and the force chains cannot experience force in any different direction other than n. Should that occur, the already existing force chains must be abandoned and new ones must be created with a different orientation that must be rejammed to support the new load [16]. This phenomenon can be observed physically by using a vacuum to remove air inside of the jamming material, causing it to become rigid. To control the stiffness of particle jamming materials, one application developed a multi-cell device consisting of hollow cells made of silicone rubber and filled with coffee grounds; after which the device was connected to a

vacuum line [68]. For multiple vacuum levels, a vacuum regulator was connected between the device and vacuum pump. To model the mechanical properties of the device while under jam, a cyclic compression test was conducted. The results of which are shown in Fig. 2.2.

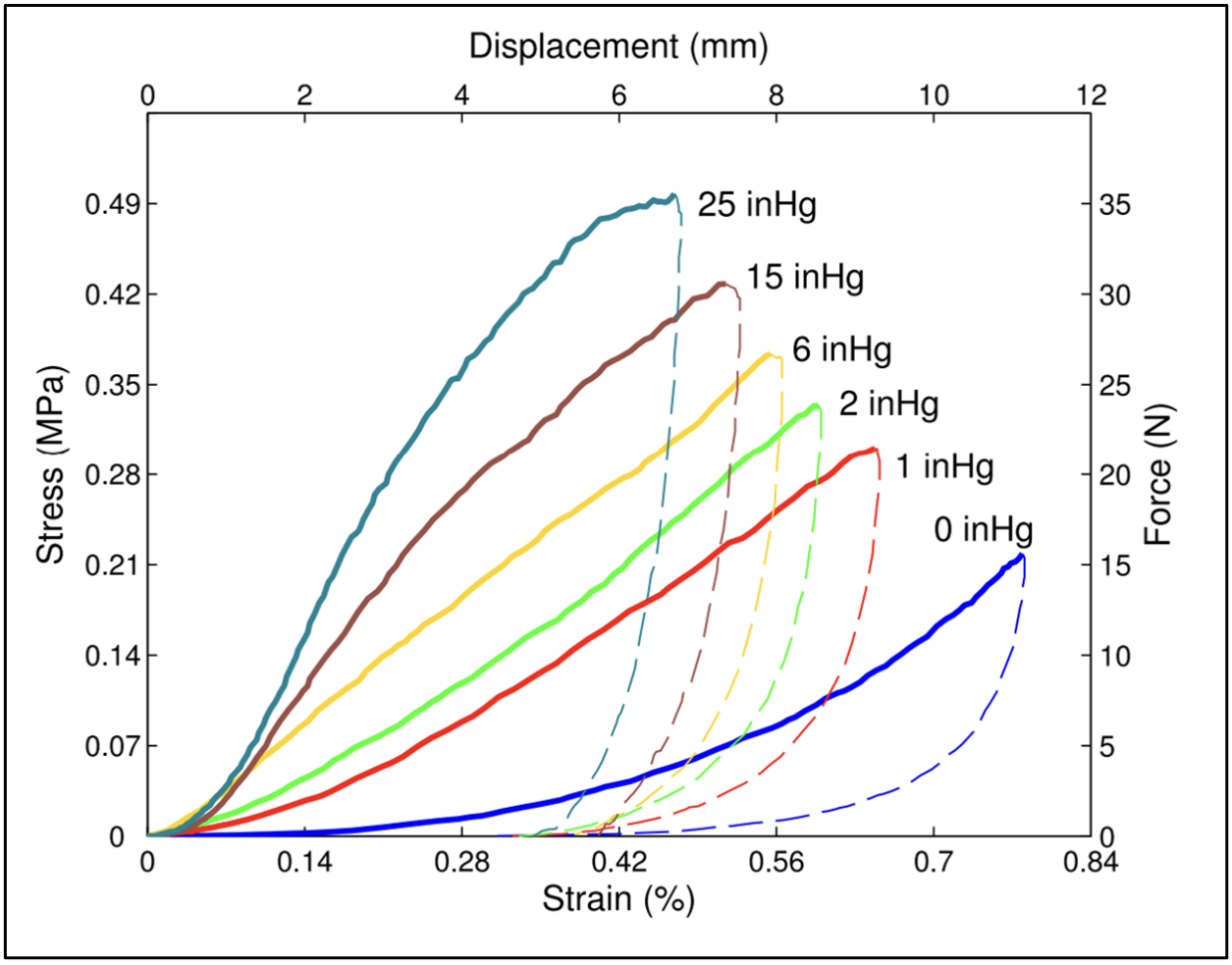

Figure 2.3: **Raw data from one sample of 10 compression trials for 6 different vacuum pressures [68] © [2015] IEEE.**

The data obtained in Fig. 2.3 indicates that the stiffness of the material is dependent on vacuum level. An advantage of jamming is that the force chains act like sets of springs connected in series because each particle can deform elastically until the applied force overcomes static friction in the least stable chains [68]. As force chains support loading along its axis

only, and therefore any large enough load on a different axis can result in rearrangement of the force chains [16, 68]. Hence, jammed materials are classified as "fragile" due to not being able to support loading on a different axis without plastic deformation [68]. Regardless, this property is useful not just for robotics and medical applications, but in other applications as well.

2.5 Granular Jamming Applications

2.5.1 Soft Robotics

Soft robotics is a subfield of robotics that is focused on the use of flexible and adaptive materials that draw heavily on biological inspiration [26]. Most research in this field is focused on utilizing jamming transition as a means of tuning stiffness [26]. This happens in any one of three ways: granular jamming, layer jamming, and fiber jamming [26]. Jamming is typically used as an actuator for stiffness-tunable mechanisms including: Electro active polymers (EAPs) (which deform under an electric field), Fluidic actuators (e.g., McKibben actuators, PneuNets), Shape memory materials (SMMs) (which can be alloys or polymers), Electro- and magneto-rheological materials (ERMs and MRMs, can be fluid or elastomers), which use embedded magnetic/electric particles that actuate under magnetic/electric field to orient and build chains (stiffen), and Low Melting Point Materials (LMPMs, alloys or polymers which display rapid stiffness change with varying temperature) [26]. Jamming provides a higher maximum stiffness than the methods mentioned above, yet it requires attachment to a vacuum pump [2, 26, 28, 40, 68, 70, 73]. Layer jamming is the least deformable, yet its restriction to non-fluidic planar sheets can easily result in internal damage done to the jamming structure when under stress, preventing areas from jamming [26]. Jamming actua-

tors force a phase transition from a fluid to a solid, yet due to the unpredictability of grains, complexity is introduced, especially in granular jamming [26]. Due to the unpredictability of grain rearrangement, reduced stability, controllability, and repeatability can occur [26]. Layer and fiber jamming can still introduce complexity from rearrangements as a result of pressure changes [26]. In soft robotics applications, device geometries and materials used play a critical role in the performance of soft robotics, especially in jamming robotics [26]. In jamming elements, the materials used are either grains, sheets, or fibers. The other area where material choices are made is the containing membrane [26]. Together, they make up a jamming actuator.

2.5.2 Aerospace Structures

Aerospace structures are a necessary part of flight control, but often penalize aerodynamic performance in the form of drag [13]. This is the direct result of surface discontinuities on the aircraft surface which are caused by mechanism based control surfaces. To reduce drag, morphing structures were explored to create smooth changes in wing shape [5, 13, 52, 72, 80]. An application of morphing structures adopts the concept of granular jamming for switchable stiffness [13]. The granular media in [13] was placed inside an elastic membrane and actuated at various pressures depending on energy requirements, and as the elastic membrane preserved the shape of the wing when the actuator was turned off, overall energy required for actuation was greatly reduced.

2.5.3 Granular Grippers

Traditional robotic grippers consist of mostly rigid joints and links [62, 63]. Actuators are placed within the links/joints/base and the grippers themselves can be equipped with sensors

that can estimate position and velocity and sensors that can gather information about its environment [62]. Despite traditional robotics grippers ranging from two-fingered models to anthropomorphic hands with fingers and a palm, there are challenges with achieving the same speed, flexibility and dexterity of a human hand when handling soft and deformable objects [62]. The "universal soft gripper" relies on a bag filled with ground coffee that grips the object by adapting to its shape [14, 62]. Even though it is capable of lifting objects such as bulbs, plastic bags, LEDs, bottle caps, and various office supplies, it cannot grasp flat objects. This is due to the coffee grounds being unable to envelop flat objects, however, it has been used in gripping applications for prosthetic [20], human robot cooperation [49, 60], and deep sea sampling [45, 62].

2.5.4 Switchable Adhesives

Adhesive bonding is essential in consumer products in the fields of healthcare, robotics, locomotion, and construction [23, 24, 30, 37, 58]. Adhesive bonding is determined by combination of interfacial properties, contact geometry, and mechanical properties which vary depending on the required application [30]. In dry environments, adhesives commonly use van der Waals forces, electrostatic forces, and hydrogen bonds to adhere to a surface [27]. When exposed to a wet or underwater environment, the aforementioned mechanisms are less effective. Regardless, in nature there are several organisms that have developed the ability to adhere to wet surfaces and in underwater environments. Organisms such as frogs, mussels, geckos, and cephalopods are known for their ability to stick to wet surfaces, as well as dry surfaces [27, 42]. Switchable adhesives are commonly used in robotic grippers for gripping and releasing objects and for sticking on wall surfaces [48]. When a material is exposed to a continuous cyclic load, crack propagation is to be expected. Strong adhesives limit crack propagation whereas reversible adhesives initiate cracks [27]. To improve crack

behavior control, switchable adhesives were developed through dynamic control of interfacial structure and rigidity [30]. An adhesive design for deterministic control consisted of a granular jamming layer made from coffee grounds, a polyethylene terephthalate (PET) backing layer, and a polydimethylsiloxane (PDMS) adhesive layer. The granular layer is connected to a pneumatic system for pressure control and surface structure tuning [30, 44, 65]. In this application, it has been shown that control of the pneumatic pressure in a granular cavity caused an increase in the stiffness interface, resulting in higher adhesive force.

2.5.5 Haptics

Haptics are defined as the technology responsible for emulating touching sensations via application of force and vibrations in a virtual environment [11, 66]. Typical virtual environments apply those forces to a stylus, thimble, or other angle for feedback, requiring the user to hold onto the end effector of the device in order to explore the physical environment [67]. To overcome this physical limitation, a tactile display with controllable geometry and mechanical properties was developed to increase the number of displayable scenarios [67, 68, 70]. As shown in Fig. 2.4, this display used a hollow layer of Ecoflex 00-30 silicone rubber (Smooth-On, Inc., Macungie, PA) filled with granular media (medium coarseness coffee grounds) connected to a vacuum line, regulated by a vacuum regulator. Underneath the silicone rubber chamber, air cylinders are connected to inflate the circular chamber before applying vacuum [69, 70].

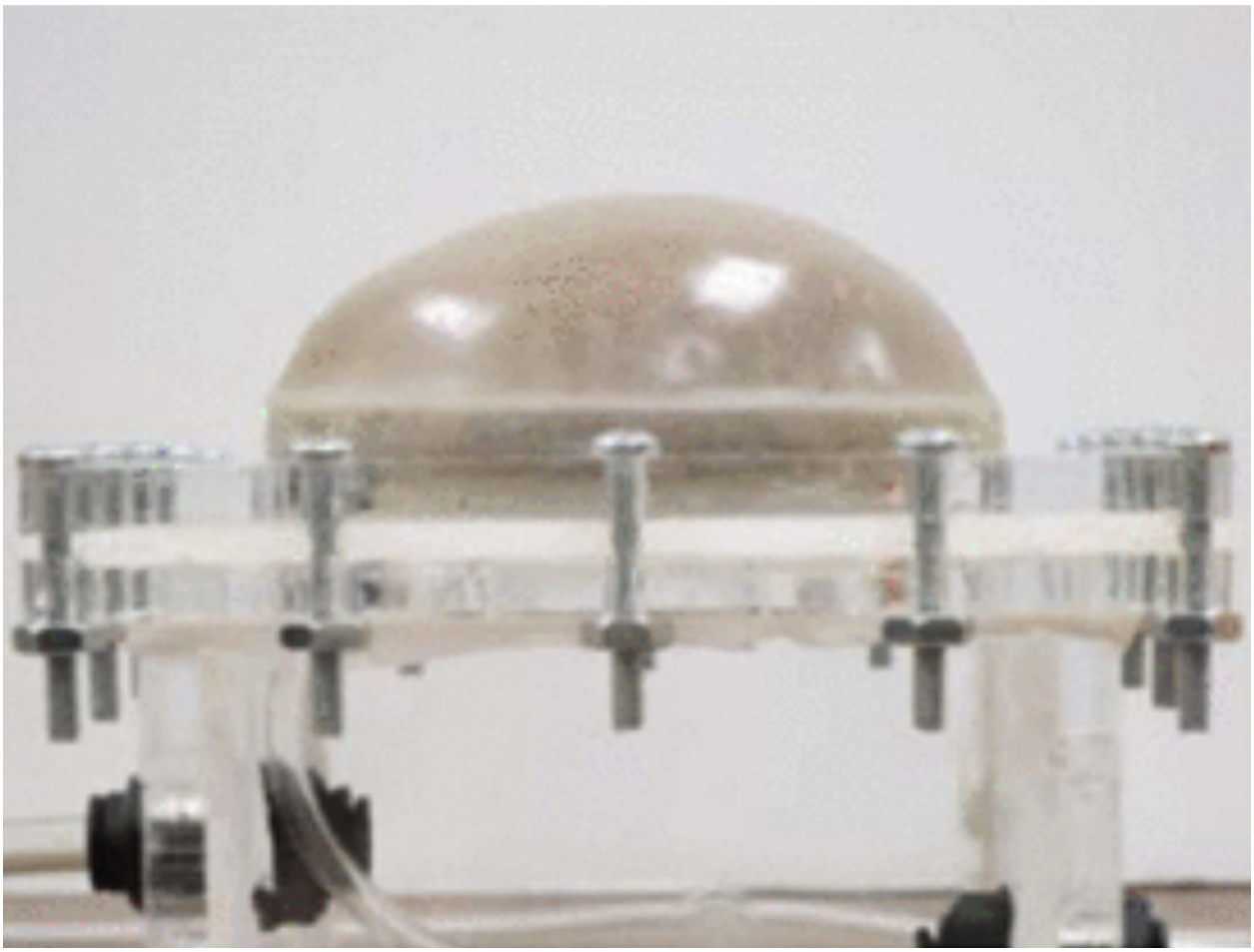

Figure 2.4: **Effects of chamber pressure on cell geometry [70] © [2013] IEEE.**

This work has been explored further by developing a controllable tactile display with increased cells [68]. As is the case for prior models of granular jamming [4, 16, 21, 46, 47], cyclic compression tests were conducted on the tactile display [68]. Six different vacuum levels, were applied to the tactile display while being subjected to compressive loading, as shown in Fig. 2.3. The results of the mechanical characterization of the tactile display showed that cell stiffness increases as the vacuum level increases, which can be used for the tunability and control of future jamming haptic interfaces [68].

2.5.6 Stiffening Garments

Robotic jamming applications have been researched for the purposes of augmenting motor performance and/or protecting the wearer's body [40]. Functional garments have traditionally been researched and explored in the sportswear, aerospace, and defense industries [40, 77]. Selective stiffening garments take inspiration from functional clothing and soft robotics to provide the user with a physiological advantage and a protective layer [40, 41].

2.6 Stiffness Tuning Methods

In this section, we review and discuss various methods used for stiffness tuning. Stiffening tuning technologies have been used for soft grippers, low-melting point alloys, electrorheological and magnetorheological fluids, and shape memory materials applications. The method of stiffness tuning was dependent on material application, as evidenced below. For instance, tendon-driven methods are also able to achieve variable stiffness through antagonistic configurations [79].

2.6.1 Electrorheological and Magnetorheological Fluids

Key components of adaptive stiffness systems are magnetorheological (MR) and electrorheological (ER) fluids, which change fluid viscosity and consequently material stiffness by applying electric and magnetic fields [57]. When exposed to an external field, these fluids change their stiffness quickly and reversibly from a fluidic to a semi-solid state. According to [57, 71], MR fluids are used in adaptive damping systems in cars to enhance ride comfort by modifying shock absorber stiffness in reaction to shifting road conditions. Comparably, ER fluids are used in robotic systems' variable stiffness joints, giving precise control over limb

stiffness and positions, improving the robot's interaction with objects of different fragilities [54, 57].

2.6.2 Tendon-Driven Systems

By using the tension in flexible tendons to change the structural rigidity of robotic components, tendon-driven systems provide a biomimetic method to stiffness tuning [56]. For robots intended to imitate the flexibility and dexterity of human limbs, a broad range of motion and variable stiffness are crucial [56, 79]. Tendon-driven actuators are widely employed in wearable exoskeletons and prosthetic devices, where they offer the compliance and stiffness required to adjust to the user's movements while maintaining comfort and safety [78]. The technology is significant because it can mimic the activities of normal muscles quite well, which makes it very useful for human-interactive robotics and other technologies that need to be highly precise and flexible.

2.6.3 Shape Memory Materials

Shape memory alloys (SMAs) and polymers (SMPs) utilize thermal and electrical stimuli to achieve major shifts in material properties [43, 50]. These materials offer a unique approach to designing self-adapting structures, as they are able to recall and revert back to their original shape when stimulated. SMAs are particularly useful in medical stents and deployable aerospace structures, where they adapt to environmental changes without external intervention [6, 22, 59]. SMPs are used in adaptive clothing that adjusts insulation properties as temperatures change, enhancing wearer comfort [81]. Shape memory materials' primary benefit is their capacity to operate independently without the need for extra mechanical parts; this capability has the potential to reduce system complexity and improve dependability.

2.6.4 Low-Melting Point Alloys

Low-melting point alloys provide facile reconfiguration of material forms by transitioning between solid and liquid phases at low temperatures [29]. This characteristic is utilized in applications that call for flexible and moldable instruments, such adaptive molds for casting and medical gadgets that have to exactly fit the anatomy of their users [8]. The capacity to recycle and reshape these materials also present substantial benefits in terms of sustainability and cost-efficiency. The main significance of low-melting point alloys lies in their potential to revolutionize manufacturing processes and medical treatments by providing highly adaptable, re-configurable solutions.

2.6.5 Microfluidic Channels and Stiffness Tuning

Microfluidic channels offer a degree of control over material properties through fluid manipulation [53]. The structure of these channels enables the dynamic modification of the fluid composition or pressure inside the microfluidic network, thus altering the mechanical characteristics of the material. This feature is critical for applications like soft robotic actuators, where high precision and complex job performance depend on precise control over material behavior [76]. To enable localized changes in stiffness and form, microfluidic channels are actually created within the elastomeric materials that make up the soft actuators. The actuator's segments can expand, contract, or stiffen without the need for rigid mechanical components by infusing or removing fluids, such as liquid or air [53]. This feature is advantageous for creating adaptive interfaces and wearable technologies that can conform to variable geometries and apply gentle forces, making them ideal for medical and assistive devices [19, 40, 69]. Furthermore, microfluidic technology's scalability makes it possible to incorporate it into smaller devices, overcoming issues with weight and size restrictions in

applications that are mobile or space-constrained. Traditional mechanical systems cannot match the precision provided by microfluidic-based stiffness control, which enables smoother transitions and more precise control over movement and force application. The precision offered by microfluidic-based stiffness control is unmatched by traditional mechanical systems, as it allows for smoother transitions and more refined control over movement and force application, highlighting its significance in the development of advanced robotic systems [76].

Chapter 3

A Granular Composite with Addressable Stiffness Utilizing Pneumatics

3.1 Abstract

One of the key functions in soft robotics is the ability to tune material stiffness. This function mimics the adaptability of natural organisms to change their rigidity to perform various tasks. One approach to rapidly tune the rigidity of a material is through granular jamming, where granular materials oscillate between fluid and solid states based on packing density alterations. We introduce a composite material, structured as a cuboid with chambers arranged in matrix configurations [12] (2x2, 3x3, and 4x4) filled with granular media. Employing a custom pneumatic system, we modulate material stiffness by selectively jamming the addressable matrix rows via negative pressure, causing changes in packing density and thus stiffness. The experimental data presents a direct relationship between the magnitude of negative pneumatic pressure and stiffness. This stiffness change is rapid and can be tuned by either adjusting the pneumatic pressure by addressing each row individually. This versatility allows for stiffness tuning across the entire material homogeneously, but also for stiffness tuning at specific material locations for heterogeneous configurations and predictive

modeling of granular composites. These capabilities open diverse ways to tune rigidity for emerging soft robotic applications.

3.2 Introduction

The development of smart materials with tunable properties is not just a rising field in the world of material science, it is the future of mechanical engineering.. These smart materials are engineered to respond dynamically to external stimuli such as electricity, heat, and magnetic fields, leading to transformative changes in their properties [18]. This capability supports advances across a range of applications, from the creation of soft, programmable materials for robotics to the development of composites with tunable stiffness for aerospace [13, 74], adhesive [27, 30], and bio-inspired applications [26]. Smart materials are capable of changing their mechanical properties in response to stimuli, resulting in applications in soft and bio-inspired robotics, aerospace engineering, and haptics [18, 61, 70]. The ability to adjust stiffness on demand provides these materials with the versatility to adapt to different operational conditions [38].

3.2.1 Granular Jamming

Granular materials are distinguished by their ability to transition between mechanically unstable and stable states as influenced by variations in key system parameters such as density, which restricts particle motion [9]. This unique property necessitates vibrations to initiate motion within these materials; as the intensity of these vibrations decreases, the materials shift from a fluid-like to a solid-like state, exhibiting yield stress [9, 30]. This behavior is not confined to granular materials alone but is also observed in soft materials

like gels [70].

Applications requiring mechanically reconfigurable parts, such as controlled locomotion and stiffness tuning, benefit significantly from the adaptability of granular materials [18]. Typically, these applications employ a design consisting of a flexible membrane or shell filled with a granular material. In its natural, unjammed state, this composite is soft, elastic, and malleable. However, upon the application of a vacuum that removes air and initiates a jamming state, it transforms into a firm, hard structure [26]. This transformation results from the formation of "force chains" among the particles, aligned with the direction of air removal.

The stability of jammed states is sensitive; even slight alterations in the direction of applied stress can disrupt the jam [46]. An illustrative example is a sand pile, which maintains its form under gravity but will yield to shifts in grain arrangement when vibrated, losing its solid-like appearance [46]. In soft robotics, the jamming mechanism facilitates considerable variations in stiffness with minimal changes in volume, supporting the development of diverse structures suited for various functionalities such as gripping, locomotion, and shock absorption in robotic limbs and end effectors [26].

3.2.2 Jamming in Soft Robotics

Most research in soft robotics is focused on utilizing jamming transition as a means of tuning stiffness [26]. This happens in three ways: granular jamming, layer jamming, and fiber jamming. Due to the unpredictability of grain rearrangement, reduced stability, controllability, and repeatability can occur [26, 39]. In robotic applications, a particle jamming part can act as a cheaper alternative for a robotic gripper where the robot presses the mass of the unjammed material around an object and then jamming it to create a rigid grip [14, 62].

In jamming elements, the materials used are either grains, sheets, or fibers. The other area where material choices are made is the containing membrane [26, 68, 70]. In granular jamming, ground coffee and man-made glass spheres are commonly used due to their availability [68].

3.2.3 Limitations of Granular Jamming Technologies

Existing granular jamming technologies face significant limitations that impact their practical application in soft robotics. These systems often struggle with mechanical complexity, particularly when hydraulic controls are employed [1], which increases the risk of mechanical failures and slows down response time. Meanwhile, soft robotic grippers have relied on controlled actuation via voltage or pneumatics [64], resulting in faster response times. However, the transition between a fluid-like and solid-like state in granular material has exhibited non-linear characteristics, making it difficult to achieve specific stiffness levels. This is due to variability in granular size and shape, which affects performance repeatability [25, 64]. To mitigate these issues, sensory feedback mechanisms have been integrated to refine control of granular applications, however, they have introduced challenges by requiring sophisticated sensors, complex system integration, and escalating costs [25]. These limitations underscore the need for research in the refinement of granular jamming technologies.

To overcome these limitations, a granular composite material with tunable rigidity is introduced. This material is designed in a variety of configurations, from a 2x2 matrix to a more complex 4x4 matrix as shown in Fig. 3.1. The multiple matrix configurations are crucial for understanding how the arrangement and density of the granules influence the stiffness of the material, which allow for the optimization of the material's performance in future soft robotics applications. Each individual chamber within these configurations is filled with

granular media and is equipped with slender tubes for the application of negative pressure [61]. To modulate the rigidity of the sample, a custom pneumatic solenoid system has been developed with the capability of selectively jamming specific rows with varying pressures [51]. To demonstrate the impact of granular positioning on the mechanical properties of the composite sample, data has been collected for the 2x2, 3x3, and 4x4 matrix configurations, comprising 4,9, and 16 chambers respectively. These findings shed light on the effects of granular jamming on this composite material, thereby enabling adjustable stiffness. The broad range of stiffness offered by this material opens up a plethora of potential applications, particularly in the growing field of soft robotics [14, 26, 82]. In addition to soft robotic gripping applications, applications for this material can be utilized in the fields of prosthetics [62], impact absorption [61], and vibration damping [70]. Furthermore, the data obtained in this study facilitate the development of predictive models that accurately estimate the stiffness of granular composite materials when subjected to varying negative pressures under controlled experimental conditions.

3.3 Methods and Setup

3.3.1 Manufacturing of Composite Material

As seen in Fig. 3.1a, the sample consists of a white Ecoflex 00-30 base, 1/8 inch polyurethane tubes, 20 gauge stainless steel tubes, coffee grounds with medium coarseness, and an upper layer of clear Ecoflex 00-30. For the 2x2, 3x3, and 4x4 matrix configurations, a custom mold was designed and 3D printed using a Bambu Labs P1S 3D Printer. Between each chamber in the mold, 1mm metal rods were inserted to create openings between chambers in the sample rows. Once the rods are inserted, the mold is sprayed with a thin layer of Easy

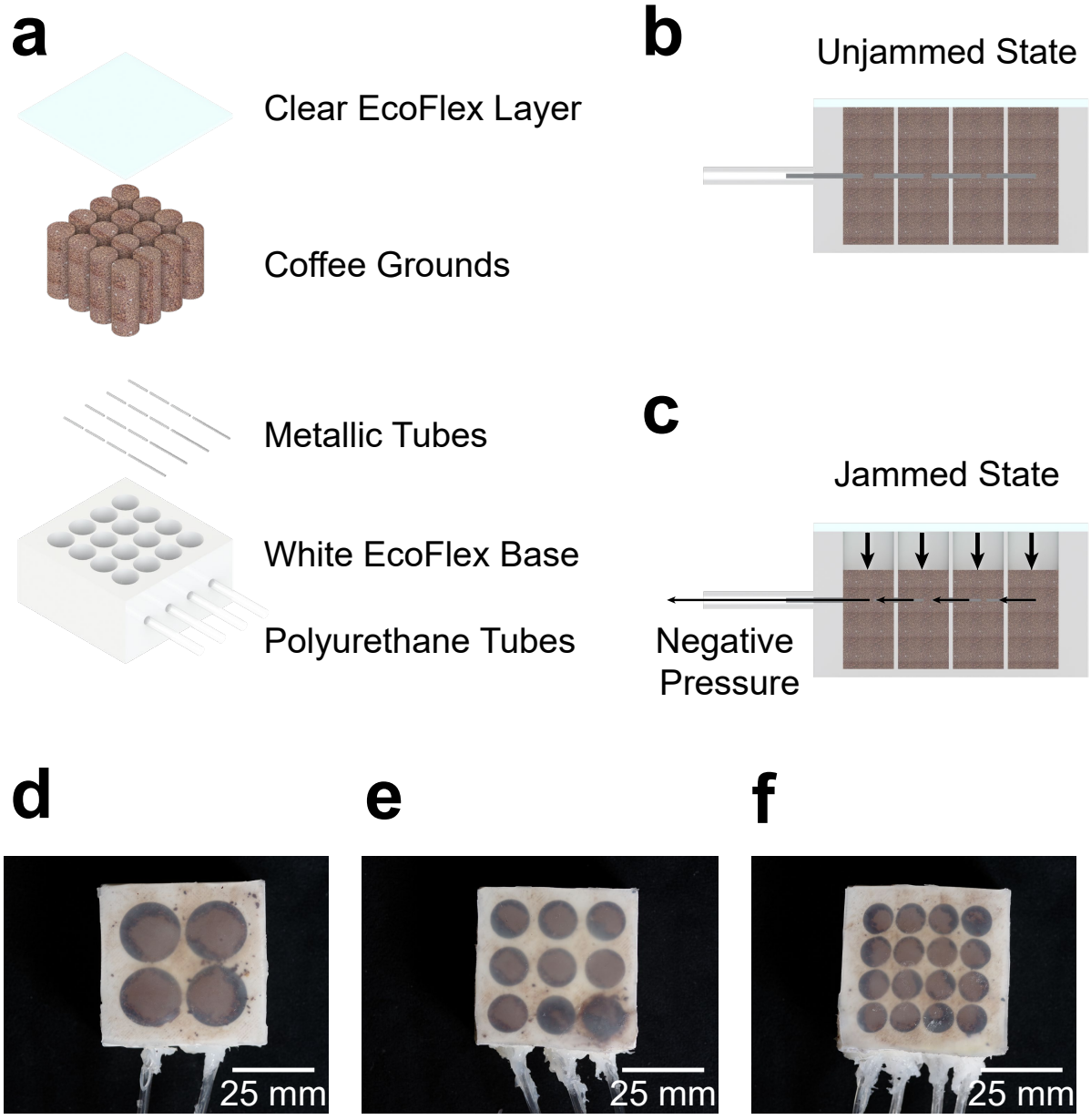

Figure 3.1: **Granular Composite Sample. a)** Sample Components **b)** Unjammed State of sample **c)** Jammed State of sample (Note that the space between coffee grounds and upper layer is much smaller than shown) **d)** 2x2 Matrix Sample **e)** 3x3 Matrix Sample **f)** 4x4 Matrix Sample

Release 200 to allow for Ecoflex 00-30 removal after curing. Ecoflex 00-30 is then made by pouring equal amounts Part A and Part B in a 1:1 ratio then pouring 1.5% total mass of

white Silc Pig color pigment. This solution is then mixed using a FlackTek DAC 1200-500 VAC SpeedMixer.

The first stage of mixing lasts for 30 seconds at a speed of 800 RPM under a pressure of 30 mBar. This is followed by a second stage of 30 seconds at 1200 RPM and 30 mBar. The third stage continues for another 30 seconds at 1400 RPM and 30 mBar. The fourth stage extends for 30 seconds at 1600 RPM and 30 mBar. The final stage of mixing is brief, lasting 10 seconds at a speed of 2000 RPM under a pressure of 990 mBar. After mixing, the Ecoflex solution is poured into the mold and left to cure at room temperature for four hours. Once cured, the metal rods are removed from the mold and the part is removed. After removal, 20 gauge hypodermic needles are cut using a Dremel 3000 and inserted into the Ecoflex part. After the needles have been inserted, 1/8 in polyurethane tubes are placed over the tubes that connect the 1st chamber of each row with the outside and are glued on using both Loctite and SIL-Poxy to ensure strong adhesion and minimal leaks. After curing for an hour, coffee grounds are poured into the chambers, with each configuration containing approximately 9.1 grams of coffee. After the coffee has been inserted, another solution of Ecoflex 00-30 is created using the process described earlier, but without the white Silc Pig color pigment. To create the clear EcoFlex layer of the sample, a small acrylic plate is covered with a thin sheet of clear film, on which the Ecoflex 00-30 is poured. Then, a film applicator (Proceq 2000 Universal Film Applicator) set to 1500 micrometers is used to apply the Ecoflex layer on the film. After application, the acrylic plate containing the clear EcoFlex layer is placed in a 40 degree oven for 15 minutes, while any remaining Ecoflex 00-30 is applied in very small amounts on the upper layer of the white Ecoflex containing the coffee grounds. Once the 15 minutes have concluded, the acrylic plate is removed from the oven and placed directly onto the sample. After four hours of curing, the clear EcoFlex layer is removed from the acrylic plate, having adhered to the sample completely. Finally, it

is then trimmed to meet the sample dimensions of 50 mm x 50 mm.

For further analysis of this granular composite material's stiffness, individual samples of white EcoFlex 00-30, clear EcoFlex 00-30, and coffee grounds were created in order to determine their Modulus of Elasticity. Since the EcoFlex 00-30 stiffness is not pressure-dependent, the ASTM D575-91 standard sample fabrication and test methods were used.

3.3.2 Pneumatic Setup

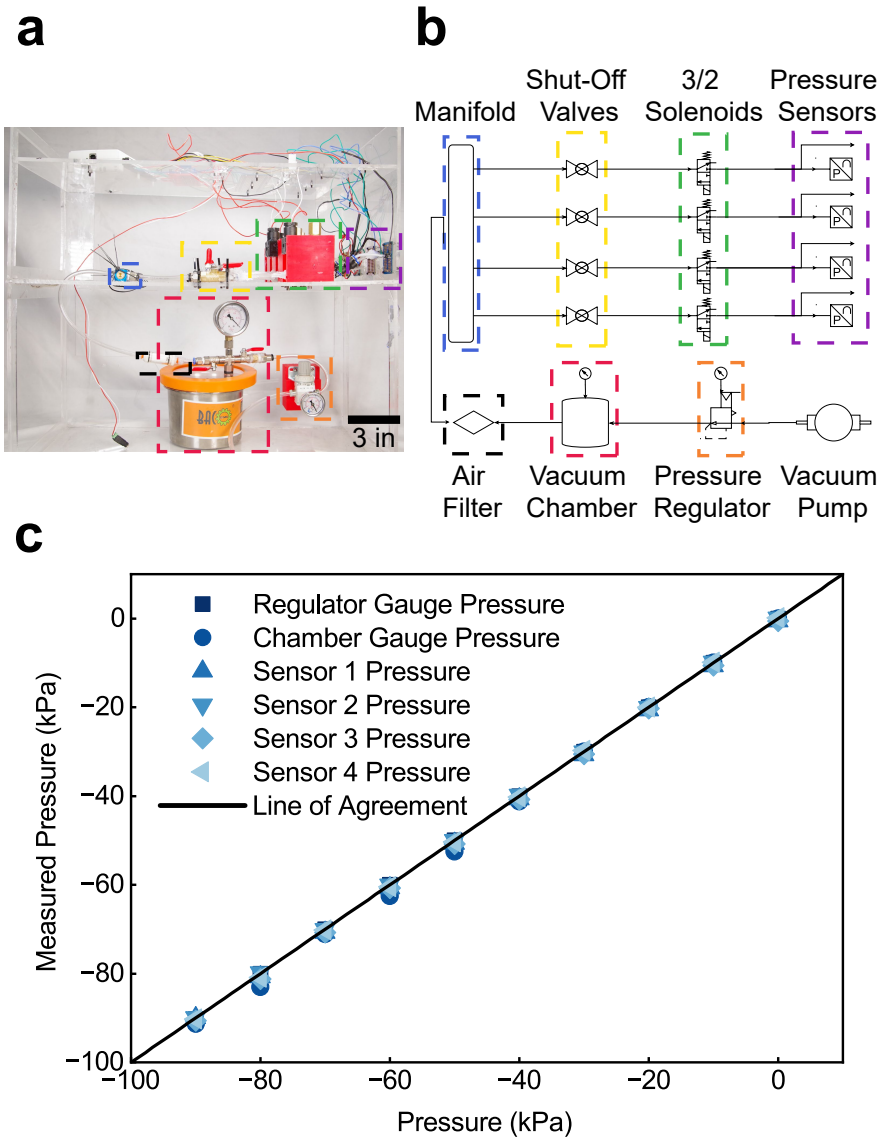

Figure 3.2: **Custom Pneumatic System. a)** Photo of pneumatic system sans vacuum pump and power supply unit **b)** Schematic of pneumatic system highlighting essential components c) Pressure calibration plot for sensors and pressure gauges.

To determine the mechanical properties of the sample, a customized pneumatic system has been designed and fabricated to trigger stiffening in each row of the sample at designated pressures as shown in Fig. 3.2. The system consists of the following: pressure regulator, cus-

tom pressure regulator mount, vacuum chamber, air filter, pneumatic manifold, four shutoff valves, four three-way two position normally closed solenoid valves, 3D printed brackets to hold the solenoids in place, 2.5 mm thick zip ties to secure the manifold and the shutoff valves, 8 mm Polyurethane tubes, 4mm Polyurethane tubes, four pressure sensors, relay, digital acquisition system (DAQ), vacuum pump, and a power supply unit.

The system is built from 1/4" thick Acrylic sheets (McMaster-Carr) that are shaped by laser cutting (Epilog Laser Fusion M2, 75 watt) into a three floor system designed to contain all components while allowing ease of access for manual control. The bottom layer shown in Figure 3b consists of a vacuum chamber, pressure regulator, air filter, 3D printed PLA mounts and M4 screws. The components mentioned are connected to each other with 8 mm polyurethane tubes. The vacuum pump is not attached to the system due to vibrations caused during its operation, and is therefore placed near the pneumatic system. The pressure regulator is directly connected to the vacuum pump, allowing for pressure level adjustment. Once the pressure level has been set, the vacuum chamber directly connected to the regulator is set to the regulator pressure, providing the system with volume to jam the sample.

Between the vacuum chamber and the pneumatic manifold, an air filter is placed to capture any stray coffee grounds from entering the vacuum pump. On the second level, the pneumatic manifold acts as a splitter, splitting the vacuum pressure to four different ports. Each of those outlets is connected to a shut-off valve, allowing for the vacuum flow to be cut off from the sample. The purpose is to fix a pressure level in one area of the sample then adjusting the overall pressure level while leaving this area unchanged, or to simply restrict the number of ports being used, such as when testing a 2x2 or 3x3 sample and needing only two ports instead of four. Next to the shutoff valves are the direct acting normally closed two position three way solenoid valves. Assuming that a sample is connected to the system, When a signal is send to these solenoid valves, the valves allow for air flow to reach the samples and

the pressure sensors. When the solenoids are closed, the negative pressure inside the sample and the sensors escapes via the exhaust port of the three-way valves. Between the solenoids and the sample, there are analog pressure sensors connected to that read the pressure.

The top layer of the pneumatic system contains the majority of the electronic components required to run the system. The pressure sensors continuously emit a signal that includes high-frequency components caused by rapid voltage changes, which can interfere with accurate data readings. To address this issue, the sensors are connected to an RC low pass filter with a cutoff frequency of 100 Hz. This filter effectively eliminates these high-frequency values, functioning like an electrical viscous damper to ensure that the data collected is more stable and reliable.

To ensure system accuracy, the pressure sensors and the gauges were recorded at specific pressure values and compared to the expected pressure. The data points in the plot shown in 3.2c represent a measurement from a different component- the pressure regulator gauge, the vacuum chamber gauge, and the pressure sensors, all measured from 0 to -90 kPa. The line of agreement illustrates where the measurements would fall if each component was perfectly accurate. Consequently, the plot proves significant accuracy for pressure across the pneumatic system.

3.3.3 Cyclic Compression Test Methodology

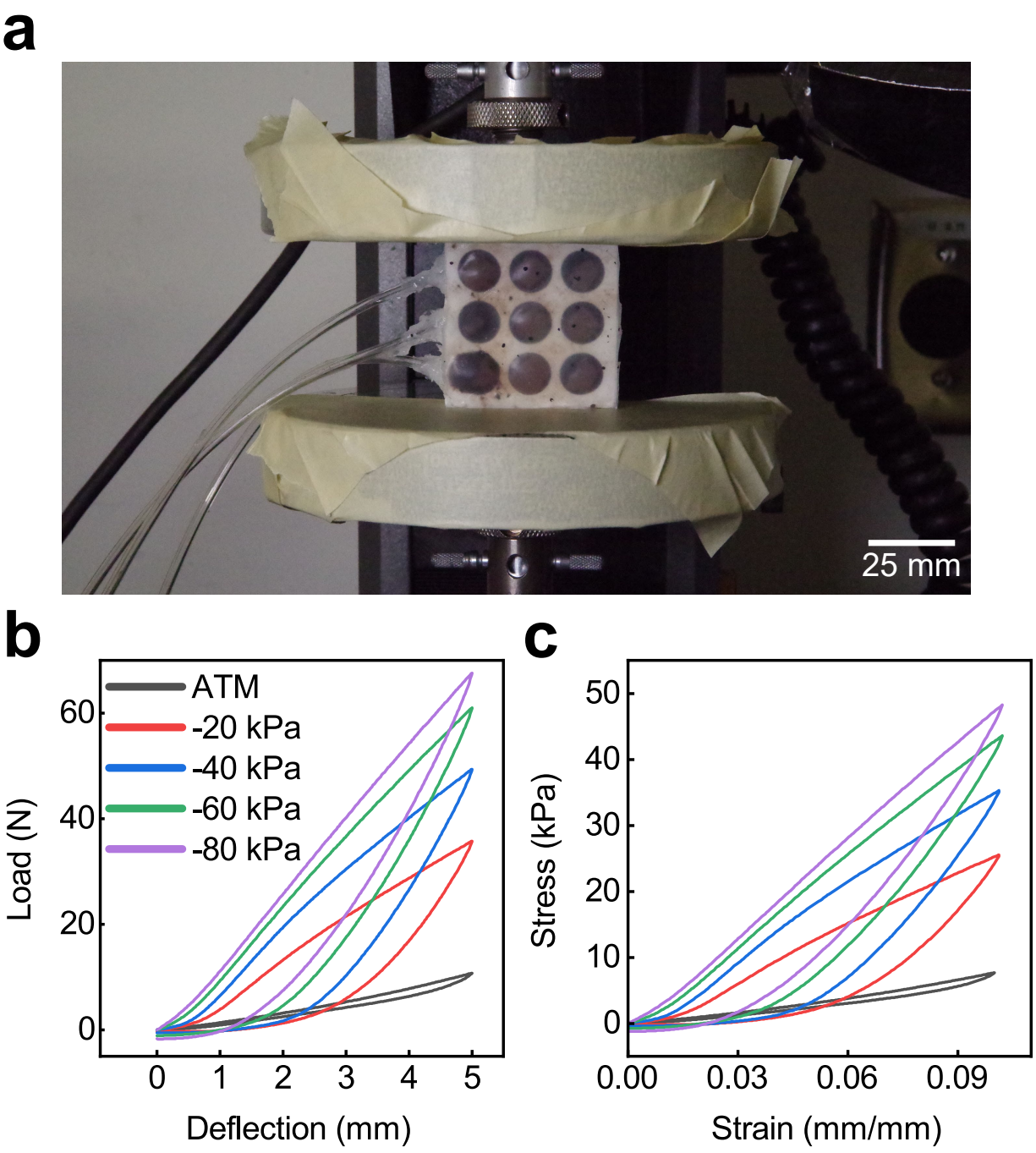

Figure 3.3: **Testing apparatus for cyclic compression test. a)** 3x3 Sample before cyclic compression test **b)** Load vs Deflection Plot at selected pressures for the 3x3 sample. **c)** Stress vs Strain Plot at selected pressures for the 3x3 sample.

Each specimen was placed in an INSTRON 5944 mechanical testing machine, between two 10 kN compression plates as shown in Fig. 3.3a for the 2x2 granular composite sample. Then a force was applied such that a deflection rate of 12 mm/min was produced until a specified deflection was reached for each specimen. After which, the force is removed from the specimen at the same rate [55]. This test was conducted for a total of three trials, and the data collected were subsequently averaged and utilized for the analyses and plots shown in this work. The specific deflection varied for each sample due to its dimensions, which are explained in more detail in the following sections.

Cyclic compression testing is crucial for understanding the mechanical properties of materials under repeated loading conditions. Below, a methodological approach to assess the reliability and precision of these tests by determining the standard deviation of Young's Modulus derived from multiple experimental trials is outlined.

Collection of Individual Measurements

In typical experimental setups, data from multiple cyclic compression tests are collected. Consider three distinct trials with the following data points:

- $(x_i^{(1)}, y_i^{(1)})$: Data from the first trial.
- $(x_i^{(2)}, y_i^{(2)})$: Data from the second trial.
- $(x_i^{(3)}, y_i^{(3)})$: Data from the third trial.

Here, i indexes the data points within each trial, where x_i might represent displacement, and y_i the corresponding force measurement.

Data Averaging Process

To synthesize a single data set from multiple trials, the mean of corresponding y-values is calculated while assuming identical x-values across the trials:

$$\bar{y}_i = \frac{y_i^{(1)} + y_i^{(2)} + y_i^{(3)}}{3}, \quad x_i = x_i^{(1)} = x_i^{(2)} = x_i^{(3)} \tag{3.1}$$

Regression Analysis

Linear regression is performed on the averaged data set $(x_i, \bar{y}_i)$ to determine the slope m, which represents Young's Modulus. The regression analysis spans the entire range of x values present in the data set, and the intercept b is not fixed, allowing it to vary to best fit the data. This approach ensures that the resulting slope m is calculated without constraints, providing a representation of the relationship between x and y.

Error Propagation and Regression

To quantify the variability and standard deviation of the slope m, error propagation techniques are employed, considering the variability in y-values [10]:

$$\sigma_m = \sqrt{\frac{\sum(y_i - (mx_i + b))^2}{(N-2)\sum(x_i - \bar{x})^2}} \tag{3.2}$$

Detailed Regression Calculations

To compute the Young's Modulus, stiffness, and their respective standard deviations, a MATLAB script was written. The script processes multiple sample data to compute averages and perform linear regression. It adjusts the regression results to align with the experimental

data and calculates the standard deviation using the methods described above.

Error analysis involves two components:

- Residuals Calculation: Represents the variability of data points around the fitted regression line.
- Spread of x-values: Normalizes the standard deviation of the slope according to the distribution of x-values.

The combined equation used in MATLAB to compute the standard deviation of the slope is:

$$\text{std\_slope} = \sqrt{\frac{\sum \text{residuals}^2}{N-2}} / \sqrt{s_{xx}} \tag{3.3}$$

3.3.4 Granular Composite Samples

As mentioned prior, the granular composite samples shown in Fig. 3.1 are 50 mm in height and length, and 28 mm in thickness. Due to the non-destructive nature of cyclic compression testing, the sample was compressed up to 5 mm of its height (10% strain). This height requirement is to minimize any plastic deformation that can occur by remaining in the linear viscoelastic range [75].

It is important that the samples are capable of being modulated homogeneously (equal pressure across all rows), selectively (one row was jammed at a time, then the next, and so on), and heterogeneously (different pressures in each row). I have defined homogeneous jamming when each row in the sample is jammed at the same negative pressure throughout the mechanical test, selective jamming is when only one row is jammed at -80 kPa throughout

the test, and heterogeneous jamming is when each row is jammed at differing negative pressures. This is allowed by using the shutoff valves to close off a row of the sample, keeping its pressure constant, while allowing the pressure to vary in other rows. In order to overcome the potential issue of granular memory, the granular composite samples were subjected to agitation between trials.

3.3.5 Individual EcoFlex 00-30 and Coffee Ground Samples

In order to understand the behavior of the granular composite material, specimens of white EcoFlex 00-30, clear EcoFlex 00-30, and coffee grounds were subjected to cyclic compression tests to determine their Young's Modulus as they are the primary components of the granular composite. The EcoFlex specimens were designed according to the ASTM D575-91 specimen dimensions, and were subjected to a cyclic compression test up to 10% strain.

Due to the brittle nature of coffee grounds, a total of nine samples of coffee grounds were prepared, one for each pressure condition. In order to run a cyclic compression test, the coffee grounds were encased in a thin layer of EcoFlex 00-30 and fabricated into a cylindrical shape as shown in Fig 3.9. The coffee grounds were subjected to a cyclic compression test up to 40% strain, but the Young's modulus measured was taken from the linear viscoelastic range from 0-10%. The reasoning behind this significant deflection was to explore any non-linear behavior beyond the linear viscoelastic region, which was not the case with the coffee ground specimens. Due to the unpredictability of grain arrangement [26], the coffee ground specimens do not share the ASTM specimen dimensions, rather, the specimen volume is the total volume of coffee grounds in my granular composite sample.

3.3.6 Predictive Stiffness Models

To formulate the predictive stiffness models, the Young's Modulus of the clear EcoFlex, white EcoFlex, and coffee grounds were recorded using the samples and methodology discussed in section 3.3.5.

Law of Mixtures

The Law of Mixtures is a method used to predict the Young's Modulus of a composite material using this equation:

$$E = E_m * \phi_m + E_d * \phi_d \tag{3.4}$$

Where E_m and E_d are the Young's Moduli of the matrix and secondary material, respectively, and ϕ_m and ϕ_d are the volume fractions of the materials [34]. This model assumes that the components of the composite material will contribute to the overall Young's Modulus proportionally to their own Young's Moduli and volume fractions. In this work, this equation is modified to account for the individual volume fractions and Young's Moduli of each row of chambers in the granular composite, the white EcoFlex material, and the clear EcoFlex upper layer of the sample. The following equations were derived using Eq. 3.4 for the 2x2, 3x3, and 4x4 matrix samples:

$$E_{2x2} = E_{EcoW}\phi_{EcoW} + E_{row1}\phi_{row1} + E_{row2}\phi_{row2} + E_{EcoC}\phi_{EcoC} \tag{3.5}$$

$$E_{3x3} = E_{EcoW}\phi_{EcoW} + E_{row1}\phi_{row1} + E_{row2}\phi_{row2} + E_{row3}\phi_{row3} + E_{EcoC}\phi_{EcoC} \tag{3.6}$$

$$E_{4x4} = E_{EcoW}\phi_{EcoW} + E_{row1}\phi_{row1} + E_{row2}\phi_{row2} + E_{row3}\phi_{row3} + E_{row4}\phi_{row4} + E_{EcoC}\phi_{EcoC} \quad (3.7)$$

The stiffness is then calculated by substituting the newly obtained Young's Modulus into equation 3.8, shown below:

$$K = \frac{EA}{h} \quad (3.8)$$

Here K is the stiffness in N/m, E is the Young's Modulus in kPa, A is the cross-sectional area in m^2, and h is the height in meters.

Spring Stiffness Model

The spring stiffness model is the division of the granular composite sample into regions, with each region considered as a spring. To build this model, two types of springs were assumed, one for the coffee grounds, and one for the white EcoFlex. This nature of this model does not account for springs in multiple dimensions, therefore only two materials are assumed for this model: the white EcoFlex, and the granular media as shown in Fig. 3.4 for the 2x2 matrix sample.

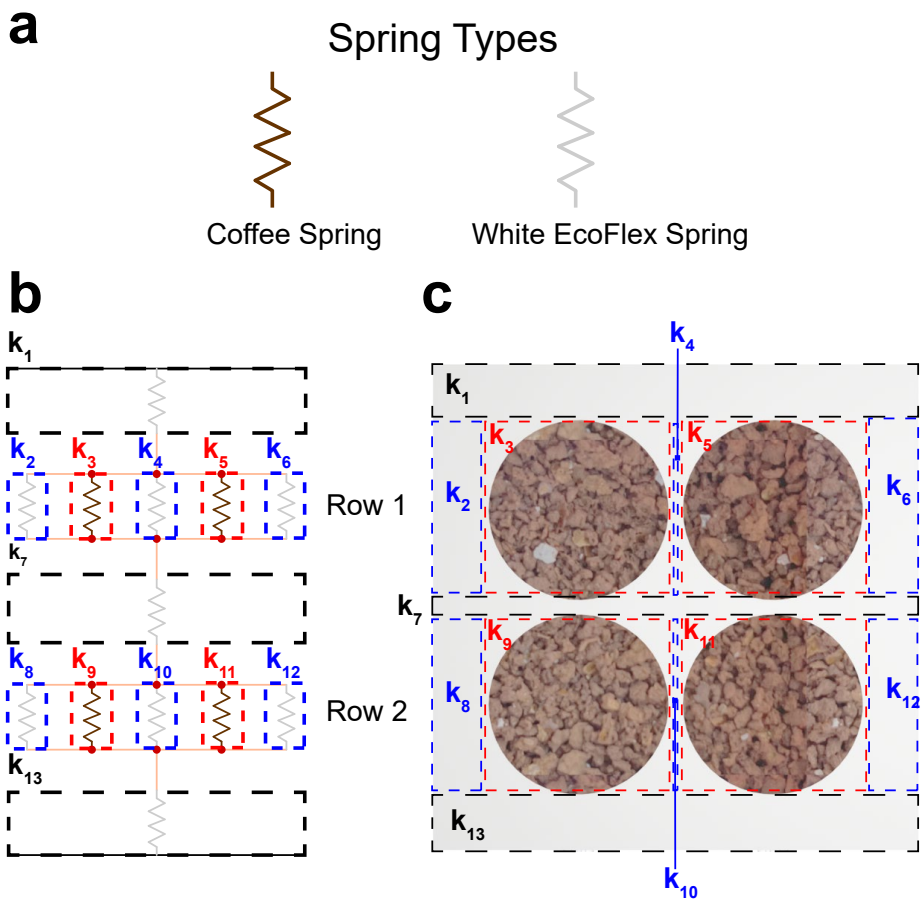

Figure 3.4: **Spring System for the 2x2 matrix sample. a)** Types of springs in spring system. **b)** Spring Stiffness Model for the 2x2 Sample. **c)** Spring Mapping for the 2x2 sample.

In the proposed model, the 2x2 sample configuration delineates thirteen distinct stiffness regions, each analogous to a spring. Regions denoted as k_1, k_7, and k_{13} consist solely of EcoFlex, illustrated in black within the schematic. Regions k_2, k_4, k_6, k_8, k_{10}, and k_{12} represent EcoFlex areas adjacent to a granular chamber along a vertical interface, highlighted in blue. Furthermore, the regions k_3, k_5, k_9, and k_{11} correspond to the granular chambers themselves, depicted in red. For simplicity, these granular chambers are modeled as rectangular zones rather than their actual cylindrical form.

The stiffness of each spring is calculated using Eq. 3.8. After computing the data, the effective stiffness of the system was found using Hooke's Law for springs in series and parallel configurations (Eq. 3.9 and Eq. 3.10).

$$\frac{1}{k_{\text{eq}}} = \frac{1}{k_1} + \frac{1}{k_2} + \ldots + \frac{1}{k_n} \tag{3.9}$$

$$k_{\text{eq}} = k_1 + k_2 + \ldots + k_n \tag{3.10}$$

Using these equations, we are able to derive a stiffness equation for the 2x2 sample shown here:

$$k_{\text{Row1}} = k_2 + k_3 + k_4 + k_5 + k_6 \tag{3.11}$$

$$k_{\text{Row2}} = k_8 + k_9 + k_{10} + k_{11} + k_{12} \tag{3.12}$$

$$k_{\text{2x2}} = \left(\frac{1}{k_1} + \frac{1}{k_{\text{Row1}}} + \frac{1}{k_7} + \frac{1}{k_{\text{Row2}}} + \frac{1}{k_{13}} \right)^{-1} \tag{3.13}$$

The stiffness calculations for the individual rows of the 2x2 granular composite sample are detailed in Equations 3.11 and 3.12 for Row 1 and Row 2, respectively. These equations provide the foundational parameters for determining the overall stiffness as articulated in Equation 3.13. Extending this analytical framework to accommodate the configurations of the more complex 3x3 and 4x4 samples necessitates adjustments for the additional granular chambers and intervening EcoFlex layers. The resultant equations for these configurations

are presented below:

$$k_{3x3} = \left(\frac{1}{k_{EcoTop}} + \frac{1}{k_{\text{Row1}}} + 2\left(\frac{1}{k_{EcoMid}} \right) + \frac{1}{k_{\text{Row2}}} + \frac{1}{k_{\text{Row3}}} + \frac{1}{k_{EcoBot}} \right)^{-1} \tag{3.14}$$

$$k_{4x4} = \left(\frac{1}{k_{EcoTop}} + \frac{1}{k_{\text{Row1}}} + 3\left(\frac{1}{k_{EcoMid}} \right) + \frac{1}{k_{\text{Row2}}} + \frac{1}{k_{\text{Row3}}} + \frac{1}{k_{\text{Row4}}} + \frac{1}{k_{EcoBot}} \right)^{-1} \tag{3.15}$$

In these equations, k_{EcoMid} denotes the stiffness of the exclusively EcoFlex regions located between the granular rows. k_{EcoTop} and k_{EcoBot} represent the stiffness of the EcoFlex regions that are positioned adjacent to the top and bottom boundaries of the sample, respectively, flanking the outermost granular rows. It goes without saying that the k_{EcoTop}, k_{EcoBot}, k_{EcoMid}, and k_{EcoRow} variables will differ for the type of sample matrix used (ex. 3x3 matrix sample).

3.4 Results

Homogeneous Jamming

The stiffness of the granular composite sample when exposed to equal negative pressure across all rows,

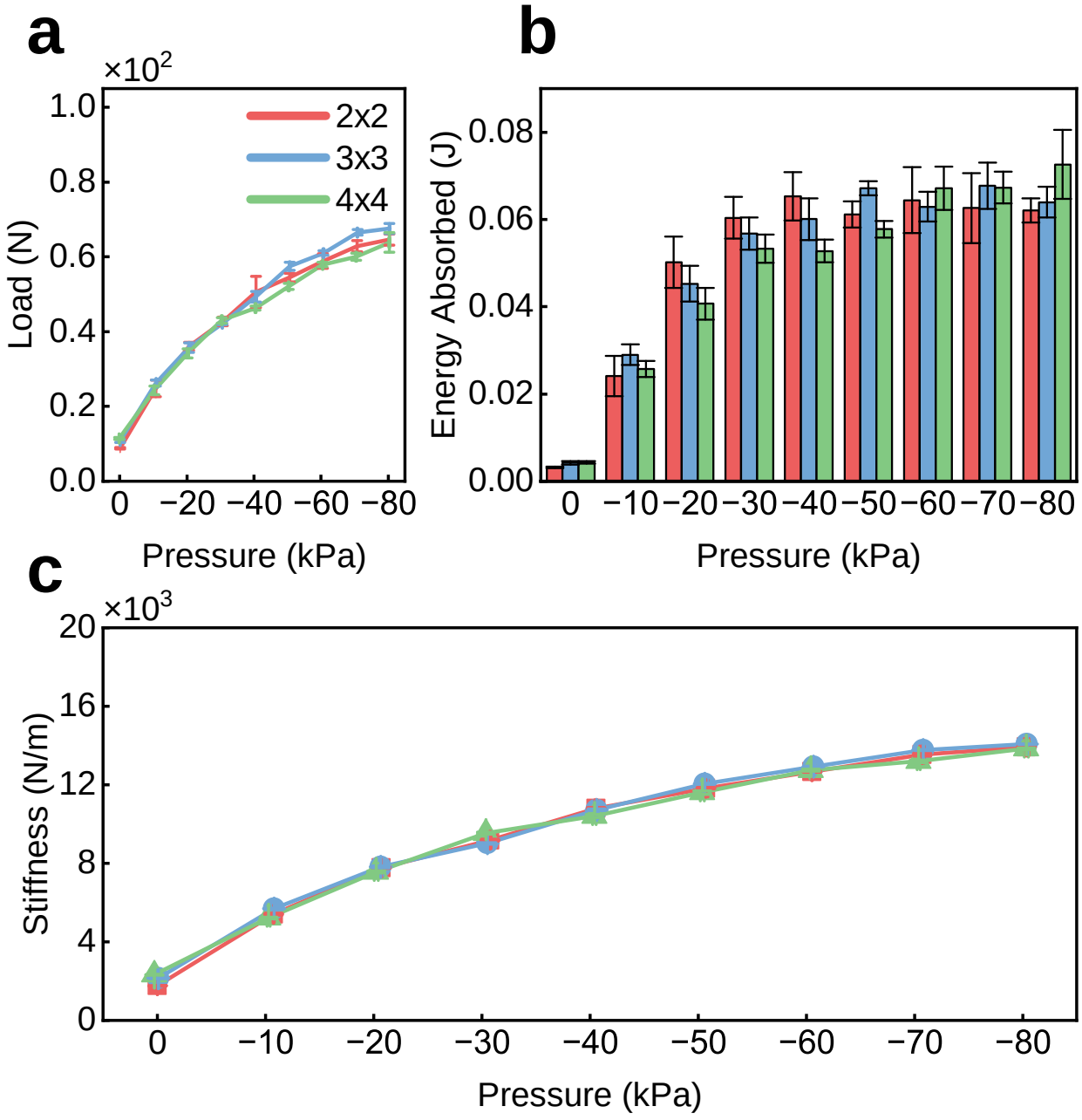

Figure 3.5: **Homogeneous Jamming.** **a)** Maximum Load vs Pressure. **b)** Energy Absorbed vs Pressure. **c)** Stiffness vs Pressure.

Fig. 3.5a provides a detailed examination of the mechanical response of the samples under varying conditions of negative pressure within the granular chambers. The samples exhibit a

significant increase in load as the negative pressure is escalated. This behavior, as graphically represented in Fig. 3.5, demonstrates the direct relationship between the applied negative pressure and the resulting stiffness of the samples. Interestingly, the samples exhibited a unique characteristic referred to as 'granular memory' between the compression cycles. Despite the agitation between cycles aimed at resetting this granular memory, the samples showed a minor decrease in load at the same deflection in subsequent cycles. This observation suggests the presence of a hysteresis-like behavior in the granular jamming process, which could have significant implications for the design and control of devices based on this material [39]. This is further evidenced upon closer inspection of Fig. 3.5b, where the energy absorbed by the samples during the test increases with pressure. The load vs pressure curves are almost linear, with the maximum load beginning to taper off at -60 kPa for all three samples.

Fig 3.5b shows that energy absorption increases as negative pressure increases. This relationship was quantified by subtracting the integral of the relaxation cycle from the integral of the loading cycle of the load-deflection curve of the cyclic compression test, an example of which is shown for the 3x3 matrix sample at selected pressures in Fig 3.3. But as load increases, so does the energy absorbed by the sample. As seen in the plot, the 2x2 matrix sample experiences significant variation compared to its 3x3 and 4x4 counterparts. This is the direct result of the 2x2 sample having more volume of coffee grounds directly acting against the compression plate during the test, resulting in higher deviation across trials for each pressure. Overall, the 4x4 sample shows slightly higher energy absorption across more pressure levels, followed by the 3x3 and 2x2 samples.

Fig. 3.5c offers a clear visualization of the direct relationship between the stiffness of the samples and the applied negative pressure. This relationship was quantified by converting to stress and strain from the averaged load and deflection data from the cyclic compression tests, then using a linear least squares fit to find the Young's Modulus of the sample, which

was then used to calculate the stiffness K using Eq. 3.8. This analysis demonstrates the direct correlation between stiffness and negative pressure, indicating the potential for precise control of stiffness in granular jamming systems through manipulation of negative pressure [39].

It is clear from the plot that stiffness increases almost linearly when negative pressure is increased, with minor deviation between the 2x2, 3x3, and 4x4 samples. This shows that the size and number of coffee chambers in a composite sample does not have any significant effect on sample stiffness when all chambers are equally jammed.

Selective Jamming

For each of the samples, only one row in the granular composite samples was kept at -80 kPa during the cyclic tests to understand the effects of variable stiffness in the samples. In the case of the 2x2 matrix sample, the top row of granular chambers was jammed at -80 kPa and the bottom row was not subjected to negative pressure of any form during the tests, as shown in Fig. 3.6. This was repeated for all granular chamber rows in the 2x2, 3x3, and 4x4 matrix samples.

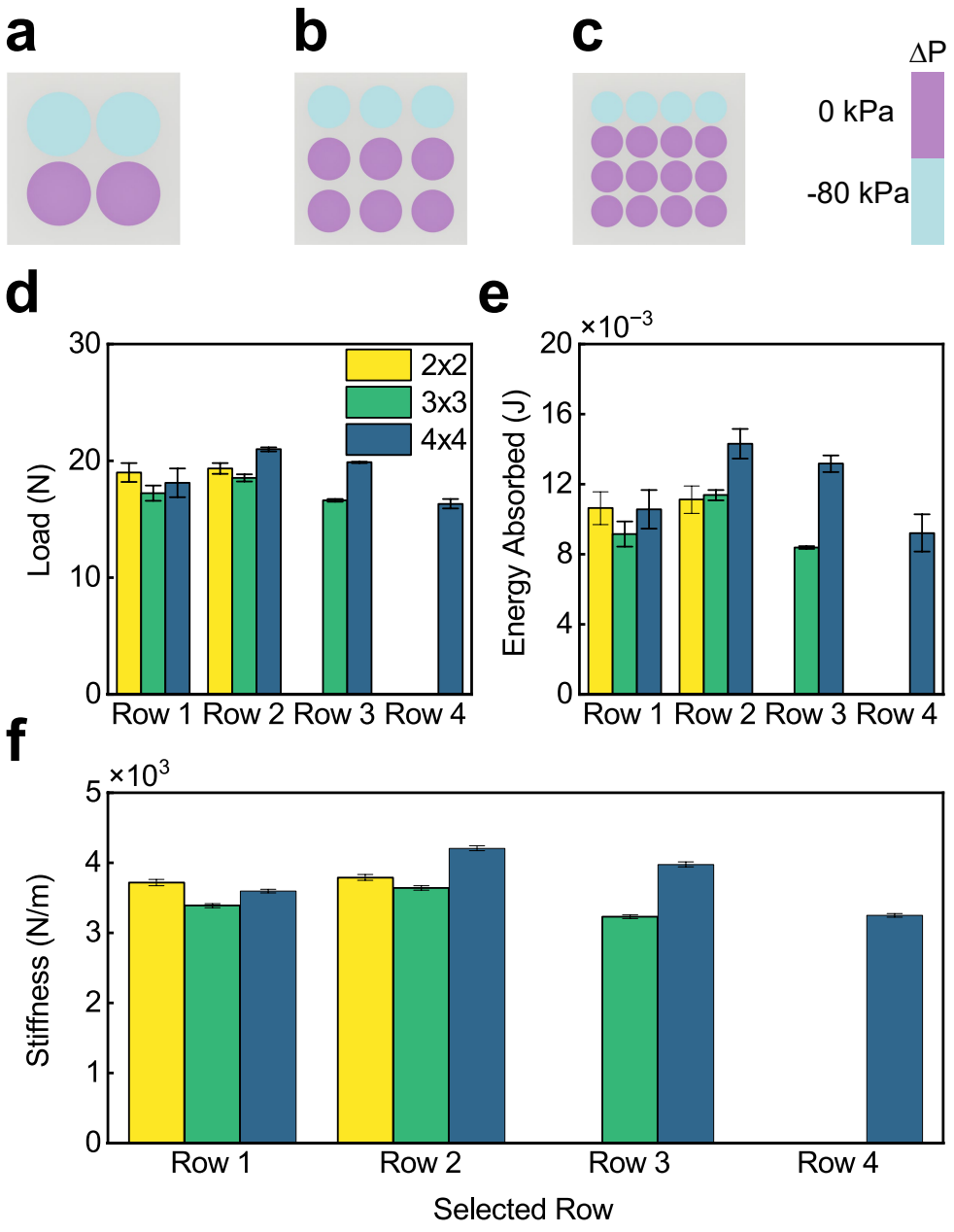

Figure 3.6: **Selective Jamming Results.** **a)** Selective Jamming Configuration for 2x2 sample. **b)** Selective Jamming Configuration for 3x3 sample. **c)** Selective Jamming Configuration for 4x4 sample. **d)** Maximum load for all samples. **e)** Energy absorbed by samples. **f)** Measured stiffness of samples.

The experimental results indicate a distinct influence of sample matrix on the mechanical

properties of the composite material when under selective jamming. The load-bearing capacity of the 2x2 sample when only one row is jammed does not vary significantly whether it is the top or bottom row that is being jammed. In the 3x3 matrix sample, the load bearing-capacity is lower than that of the 2x2 and 4x4 samples due to the lower volume and arrangement of jammed granular media. Notably, the second row is the 3x3 sample bears the highest load, indicating that the position of the jammed granular media can affect load bearing. The 4x4 sample has higher load-bearing capacity than the 3x3 sample, which is due in part to the closeness of the granular chambers in each row. Notably, the middle rows in each configuration result in the sample bearing the highest load, which suggests that the stiffening effect of granular jamming extends slightly to the surrounding EcoFlex regions between the jammed and unjammed rows. Stiffness measurements are exhibiting the same trend shown in the load sub-figure in Fig. 3.6f. When comparing the results of the top and bottom rows of the 3x3 and 4x4 samples, it is clear that load-bearing capacity does not differ.

In terms of energy absorption, a similar pattern to the load plot is present. The 2x2 sample absorbs the same amount of energy during the cyclic test regardless of jammed row, whereas the 3x3 and 4x4 samples absorb more energy when the middle row is jammed (or in the case of the 4x4, the second and third row). Interestingly, the samples with the highest energy absorption and load bearing capabilities indicate higher effectiveness at energy dissipation.

Heterogeneous Jamming

To understand the effects of varying negative pressure on stiffness and energy absorbed, the 2x2, 3x3, and 4x4 matrix samples are jammed in multiple configurations to better understand the effect of pressure variation on overall sample stiffness stiffness. The jamming conditions are shown in Fig. 3.7.

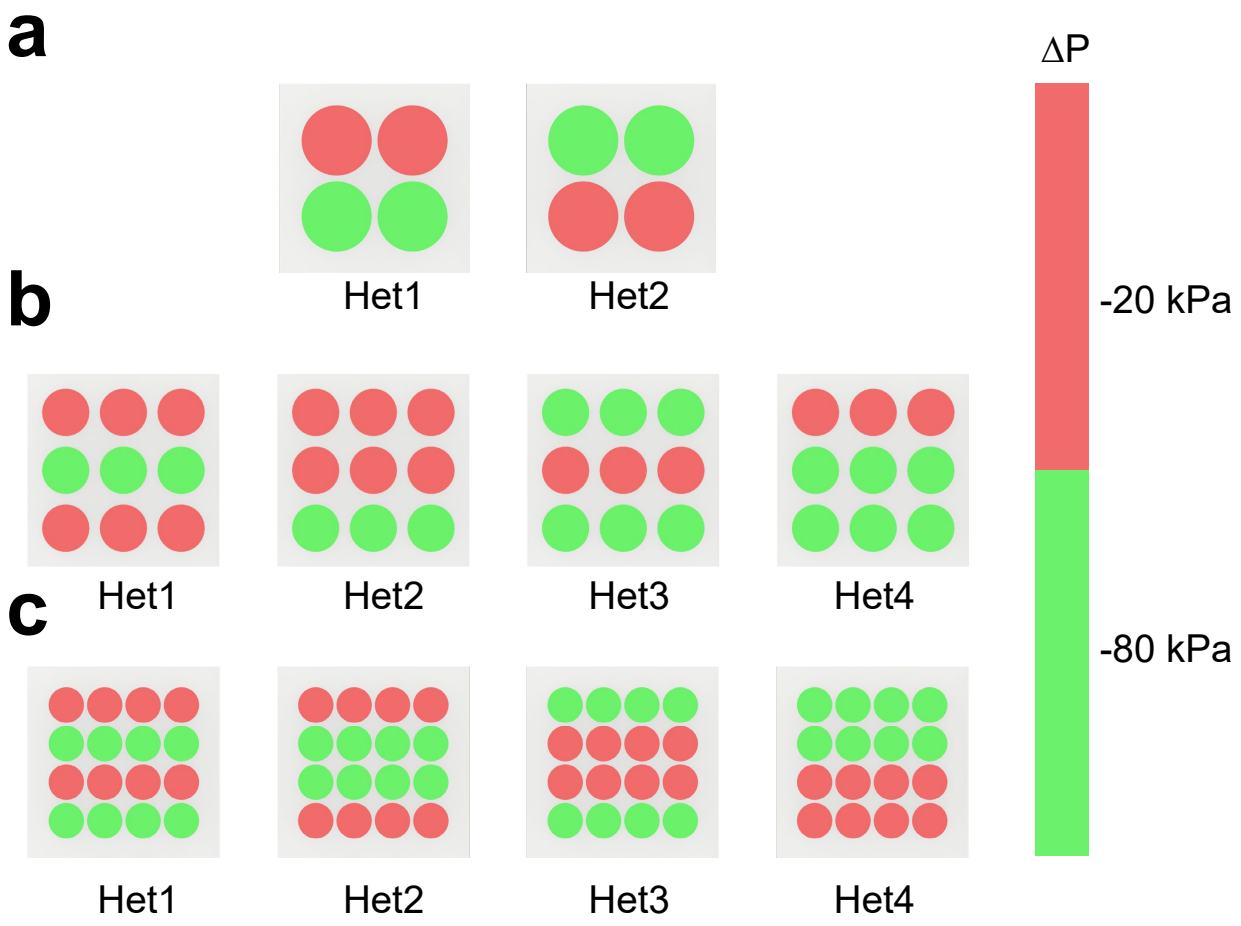

Figure 3.7: **Heterogeneous Jamming Sample Configurations. a)** 2x2 Sample Heterogeneous Jamming Configurations. **b)** 3x3 Sample Heterogeneous Jamming Configurations. **c)** 4x4 Sample Heterogeneous Jamming Configurations.

In Fig. 3.7a, the 2x2 sample is heterogeneously jammed, with one row at -20 kPa and the other at -80 kPa. Similar to the selective jamming, the sample has two configurations, with the bottom row being jammed at a higher pressure and the top row at a lower pressure. In this sub-figure, we see two heterogeneous configurations for the 2x2 sample, labelled Het1 and Het2. For the 3x3 sample shown in Fig. 3.7b, the 3x3 sample has four different jamming configurations. Het1 and Het2 in the 3x3 sample have an average pressure of -40 kPa, with

two rows at -20 kPa and one row at -80 kPa, whereas Het3 and Het4 have an average pressure of -60 kPa, with one row at -20 kPa and the others at -80 kPa.

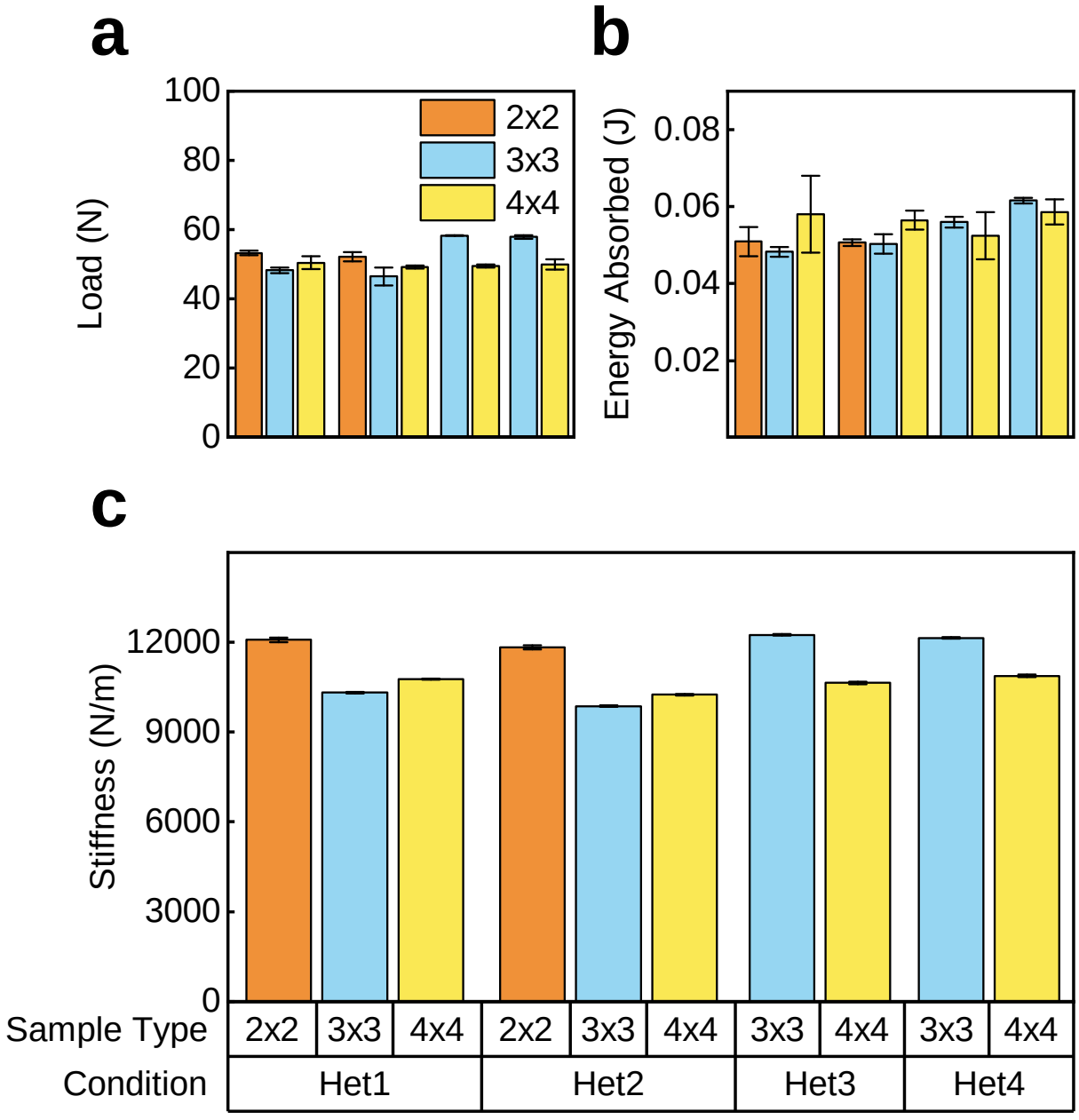

Figure 3.8: **Heterogeneous Jamming Results. a)** Load vs Jamming Configuration Plot. **b)** Energy Absorbed Plot. **c)** Stiffness Plot.

In Fig. 3.8a, we observe the load-bearing capacities across various sample configurations.

Previous investigations for selective jamming, detailed in Fig. 3.6, have demonstrated that the 2x2 sample configurations, specifically Het1 and Het2, exhibit comparable trends in their load-bearing capabilities. Similarly, for the 3x3 sample, configurations Het1 and Het2 display closely aligned load capacities, although Het2 shows a marginally reduced capacity and greater variability across different trials. This is also the case for the 3x3 Het3 and Het4 configurations. Notably, the 4x4 sample under heterogenous jamming conditions possess load capacity that, while lower than those observed in the 2x2 configurations, exceed the capacities of the 3x3 Het1 and Het2 configurations. In Fig. 3.8c, the 2x2 sample heterogenous configurations have higher stiffness than its 3x3 and 4x4 heterogeneous counterparts, with the exception of the Het3 and Het4 jamming configurations for the 3x3 sample. This plot follows the same trend that is apparent in Fig. 3.8a.

In Fig. 3.8b, it is clear that the 4x4 heterogeneous configurations absorbed more energy than the 2x2 and 3x3 Het1 and Het2 configurations, despite having a lower load-bearing capacity. This behavior is explained by the hysteresis of the samples after experiencing compression. As these samples are subjected to repeated testing, with agitation between tests, granular memory can manifest depending on the stress history of the sample. The particles inside the granular media can rearrange themselves in such a manner that retains information about past stress, influencing future structural stability [35, 39]. Upon closer inspection of the 4x4 heterogeneous configurations, the granular media inside of the samples experienced small temporary deformation that resulted in higher deviation during the relaxation cycle of the cyclic loading test, resulting in higher deviation of energy absorbed across multiple trials.

Interestingly, the Het1 and Het2 configurations of 2x2 and 3x3 samples exhibit a reduced capacity for energy absorption, coupled with lower variability across test trials. This phenomenon is primarily attributed to the relatively subdued load conditions encountered during testing, which is evident in the 3x3 Het1 and Het2 configurations. Conversely, the 2x2 con-

figurations demonstrated marginally higher energy absorption capabilities compared to their 3x3 counterparts. Despite these differences, the deviation between the 2x2 and 3x3 Het1 and Het2 configurations remains minimal, suggesting a consistent behavior pattern within this experimental range.

3.4.1 Model Comparison and Validation

The stiffness predictive models have been developed to estimate the stiffness properties of granular composite materials, specifically under controlled testing conditions and multiple jamming conditions. To validate these models, a series of cyclic compression tests were executed across a range of material specimens that make up my samples, including clear EcoFlex 00-30, white EcoFlex 00-30, and coffee grounds. These tests were used to determine the respective Moduli of Elasticity for each type at the linear viscoelastic range from 0 to 10% strain, as shown in Fig. 3.9. Detailed methodologies pertaining to the experimental setup, test execution, and calculations for the Young's Modulus are provided in Section 3.3.

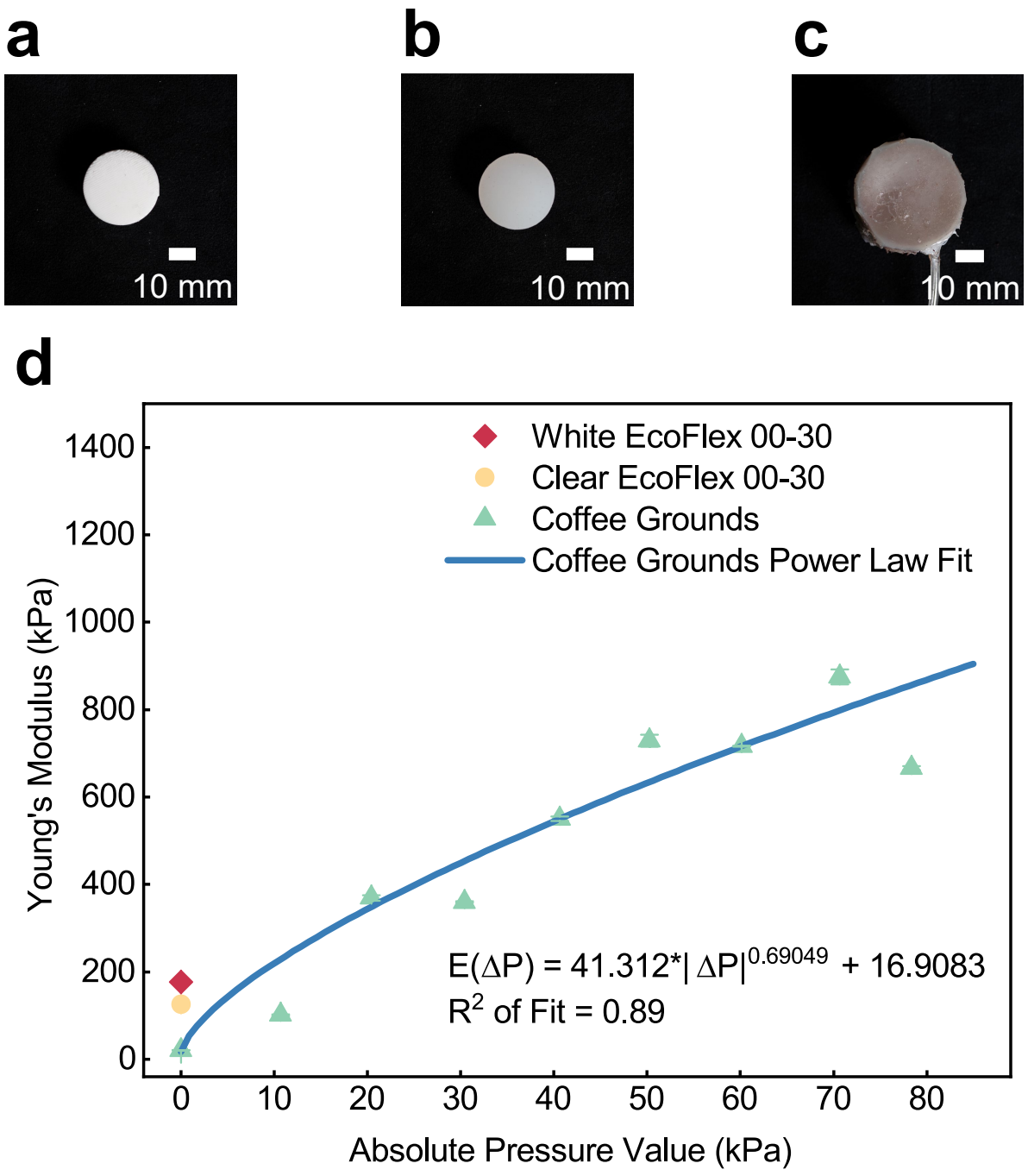

Figure 3.9: **Individual Material Young's Modulus Measurements. a)** White EcoFlex 00-30 ASTM specimen. **b)** Clear EcoFlex 00-30 ASTM specimen. **c)** Coffee Ground specimen. **d)** Pressure vs. Young's Modulus for material specimens.

In Fig 3.9d, the elastic properties of both the white and clear EcoFlex 00-30 samples are depicted, demonstrating minimal difference in values. That divergence between both values can be attributed to the inclusion of white Silc-Pig in the white EcoFlex sample, which enhanced its modulus. The coffee grounds exhibit a more complex response under compression. As this sample is subjected to varying levels of negative pressure, a nonlinear increase in stiffness is present. To characterize this behavior, a power law function is fitted to this data, providing a model that adapts to the range of pressures from 0 to -80 kPa. Since the power law function does not accommodate negative values, absolute pressure values were necessary. For instance, when a granular specimen is jammed at -60 kPa, it is represented as 60 kPa in the function to align with the mathematical requirements of the power law function, which does not accept negative values. Furthermore, the stiffness models built on the Law of Mixtures and the Spring System assumption utilize the power law function depicted in Fig. 3.9 to calculate the Young's Modulus of granular media under specific pressures. These values are then integrated into the respective equations for each sample configuration and chosen stiffness model- equations 3.5, 3.6, 3.7, 3.13, 3.14, and 3.15. Each formula is derived to reflect the specific jamming state of the sample, whether it be homogeneous, selective, or heterogeneous.

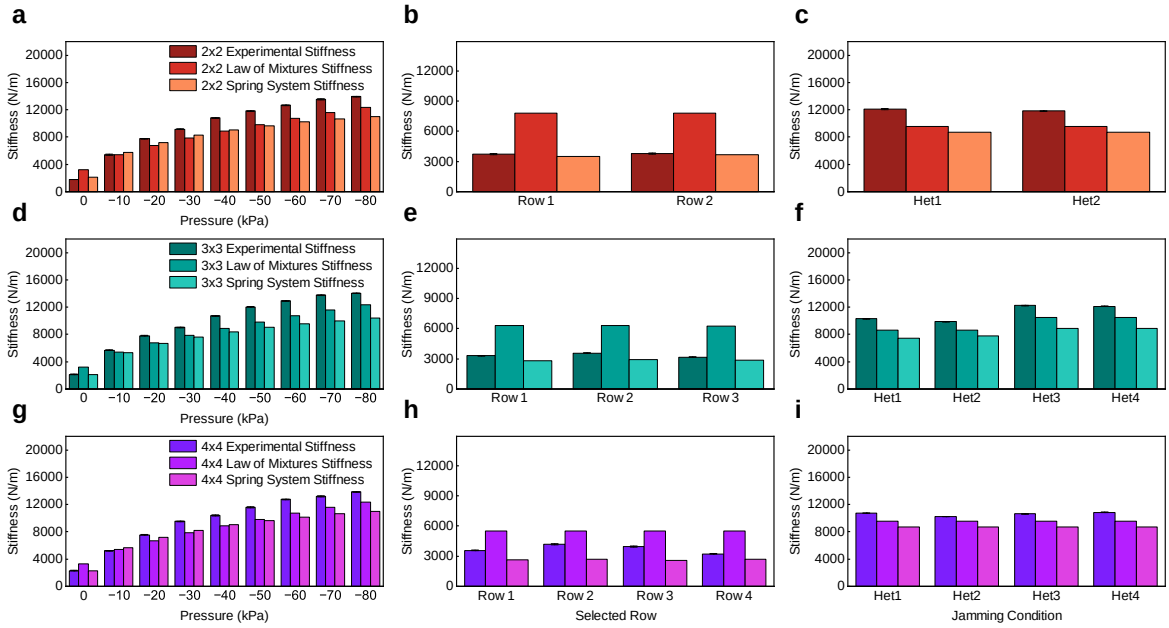

Figure 3.10: **Stiffness Model Comparison for Homogeneous, Selective, and Heterogeneous jammed samples. a)** Stiffness vs Pressure for experimental and model data for 2x2 matrix sample under homogeneous jamming. **b)** Stiffness vs Selected Jammed Row for experimental and model data for 2x2 matrix sample under selective jamming. **c)** Stiffness vs Jamming Condition for experimental and model data for 2x2 matrix sample under heterogeneous jamming. **d)** Stiffness vs Pressure for experimental and model data for 3x3 matrix sample under homogeneous jamming. **e)** Stiffness vs Selected Jammed Row for experimental and model data for 3x3 matrix sample under selective jamming. **f)** Stiffness vs Jamming Condition for experimental and model data for 3x3 matrix sample under heterogeneous jamming. **g)** Stiffness vs Pressure for experimental and model data for 4x4 matrix sample under homogeneous jamming. **h)** Stiffness vs Selected Jammed Row for experimental and model data for 4x4 matrix sample under selective jamming. **i)** Stiffness vs Jamming Condition for experimental and model data for 4x4 matrix sample under heterogeneous jamming.

The analysis provided in Fig. 3.10 encapsulates a comparative study of the stiffness of the 2x2, 3x3, and 4x4 granular composite samples under homogeneous jamming conditions. For all matrix configurations, the experimental stiffness values serve as a benchmark for assessing the accuracy of the Law of Mixtures and Spring System models. As shown in Fig. 3.5, the samples are subjected to a gradient of pressures from 0 to -80 kPa. The experimental results of the cyclic compression tests are compared to the predictive results using the Law

of Mixtures model and the Spring System model at the same pressures. In sub-figures a, d, and g, there is a clear trend of increasing stiffness with increasing negative pressures for the predictive models.

The Law of Mixtures model has a tendency to underestimate the stiffness at pressures lower that of the atmosphere by a difference of 2% - 16% for pressures set to -10 kPa and lower, whereas the spring system model underestimates the stiffness at those pressures by a difference of 2% - 25%, depending on the sample type and pressure. These observations suggest that both stiffness models do not fully encapsulate the complex interactions present within the granular media and the surrounding EcoFlex matrix. Another contributing factor to the differences between the experimental and model data is the inherent unpredictability of the coffee samples used for the predictive model's granular stiffness. As cited in previous papers, this scenario is typical for granular jamming applications [25, 64].

Unlike the homogeneous jamming conditions shown in subfigures a,d, and g, the Law of Mixtures model overestimates sample stiffness by a significant margin, ranging from 31% to 114% in some cases. The Spring System model, however, captures the stiffness response of the granular composite material under the same jamming conditions more accurately.

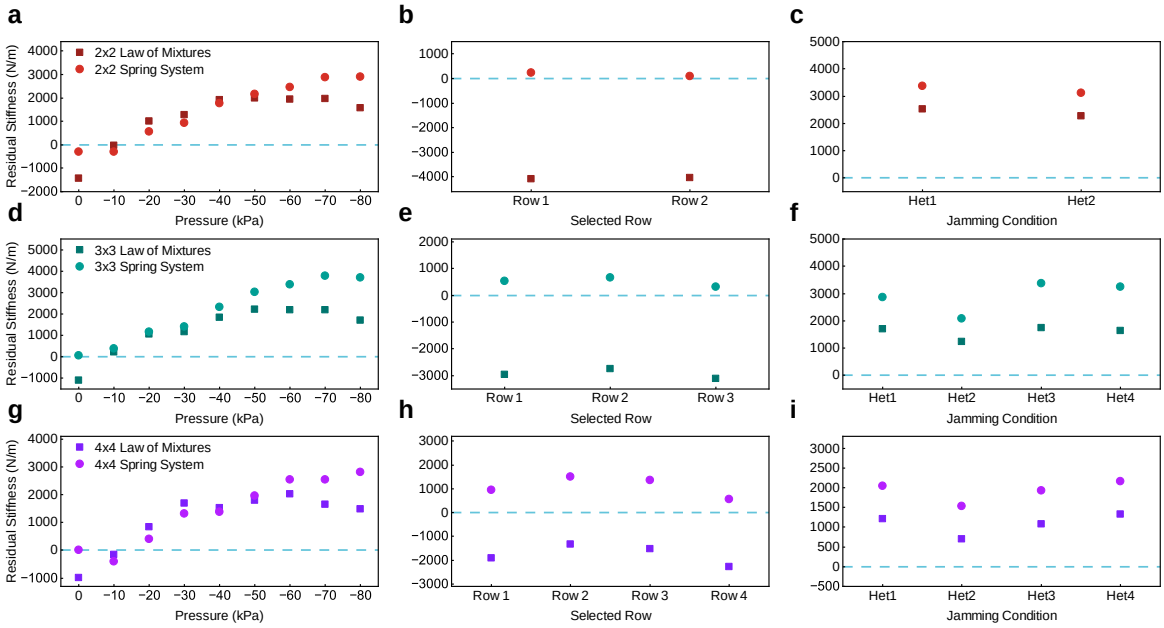

Figure 3.11: **Residual Stiffness Plots for Homogeneous, Selective, and Heterogeneous jammed samples. a)** Residual Stiffness for 2x2 matrix sample experimental and model data under homogeneous jamming. **b)** Residual Stiffness for 2x2 matrix sample experimental and model data under selective jamming. **c)** Residual Stiffness for 2x2 matrix sample experimental and model data under heterogeneous jamming. **d)** Residual Stiffness for 3x3 matrix sample experimental and model data under homogeneous jamming. **e)** Residual Stiffness for 3x3 matrix sample experimental and model data under selective jamming. **f)** Residual Stiffness for 3x3 matrix sample experimental and model data under heterogeneous jamming. **g)** Residual Stiffness for 4x4 matrix sample experimental and model data under homogeneous jamming. **h)** Residual Stiffness for 4x4 matrix sample experimental and model data under selective jamming. **i)** Residual Stiffness for 4x4 matrix sample experimental and model data under heterogeneous jamming.

This is confirmed via the Residual Stiffness plots shown in Fig. 3.11 for the Law of Mixtures and Spring System stiffness. The residual plots show the measured difference between the experimental stiffness data and the stiffness model data for both the Law of Mixtures and Spring System methods for the 2x2, 3x3, and 4x4 samples under the specific jamming conditions (homogeneous, selective, and heterogeneous). For the homogeneously jammed samples, the residual stiffness increases with negative pressure. This indicates that the models' underestimation of sample stiffness is due to not accounting for the interactions with the

composite material.

Focusing on the 2x2 matrix sample in sub-figure b, the spread between the zero line and the Law of Mixtures is quite broad, indicating that it is unable to capture the stiffness behavior of the granular composite when one row of the sample is jammed at -80 kPa and the other is left untouched. The variability presented by the plot suggests that the model does not account for interactions within the composite material. Sub-figures e and h for the 3x3 and 4x4 samples exhibit similar trends in regards to the significant residuals, but at a slightly smaller range. The spring system stiffness shown in sub-figures b, e, and h present a smaller residual stiffness, indicating a more accurate fit compared to the Law of Mixtures when selectively jammed. This is evidenced by the closeness of the stiffness values of the experimental and spring system model shown in the bar plots in sub-figures a, d, and g.

The residuals shown for the 2x2 sample in sub-figure b are in close proximity to the zero line, indicating accurate predictive capability of the spring system model for the 2x2 matrix sample. A similar trend can be scene in sub-figure e, for the spring system stiffness pertaining to the 3x3 sample. The residual is small, yet the value is noticeably larger than that of the 2x2 sample. Despite this, the residual stiffnesses are clustered close to the zero line, suggesting effective modeling of stiffness behavior. These observations can be extended to the 4x4 sample shown in sub-figure h, with a larger residual stiffness. This behavior can be explained by the 3x3 and 4x4 sample having more complex geometry, thereby increasing variability.

Overall, the Spring System model demonstrates a consistency for accurate stiffness prediction of granular composite samples that when under selective jamming conditions that isn't present with the Law of Mixtures stiffness model. The residual plots illustrate these points, and while the model is generally viable, there is clearly a demonstrated need for more complex modelling to better capture the granular composite behavior.

When the samples are heterogeneously jammed, the Law of Mixtures and Spring System models both underestimate the overall sample stiffness similar to the homogeneous jamming data in Fig. 3.10 and 3.11. For the 2x2 matrix sample in sub-figure a, there is a noticeable underestimation of stiffness by both models, with the Law of Mixtures showing a greater disparity from the experimental measurements than the Spring System. It is clear from sub-figures a-c that both models underestimate stiffness for the 2x2 sample when heterogeneously jammed. In sub-figures d-i for the 3x3 and 4x4 samples, the underestimation pattern persists, but the deviation between experimental and model stiffness grows larger. This is directly attributed to the increased complexity of the granular media and its interactions within the sample material.

Sub-figures c, f, and i in Fig. 3.11 focus on the residual stiffness between the experimental results, Law of Mixtures, and Spring System predictions across the three sample configurations. The consistent underestimation across all sample matrices highlights a systemic limitation within the Law of Mixtures model when applied to heterogeneous jamming scenarios. In contrast, the Spring System model's performance shows a relatively larger spread of residuals and a greater deviation from the experimental measurements. This indicates that the Spring System model, while not perfect, provides a less reliable stiffness prediction under heterogeneous jamming conditions.

Across all jamming conditions, it is evident that the spring system model generally offers better predictability and adaptability for all jamming conditions of the granular composite compared to the Law of Mixtures model. However, both models experience limitations in accurately capturing the stiffness of granular composite samples under non-jamming conditions. Observations indicate that the Law of Mixtures model tends to underestimate stiffness, potentially due to its simplifying assumptions that do not fully account for the nonlinear interactions between the granular components and the matrix material. In contrast, the

Spring System model, which conceptually integrates the granular and EcoFlex interactions through a network of spring-like connections, exhibits a closer alignment to the experimental data, despite underestimating the sample stiffness. The selective and heterogeneous jamming conditions reveal gaps in both models, particularly in accounting for the interactive effects of granular media mixed with compliant EcoFlex matrices.

3.4.2 Stiffness Tunability between Homogeneous and Heterogeneous Jamming

The provided figure comprises three sub-figures (a, b, c), each illustrating the stiffness characteristics of granular composite samples under various heterogeneously jammed conditions, across three different matrix configurations: 2x2, 3x3, and 4x4. Each panel represents the experimental stiffness values, the predicted stiffness by the Law of Mixtures model, and the Spring System model, respectively. The dotted line in Fig. 3.12 represents the homogeneously jammed sample stiffness at the average pressure of the homogeneous and heterogeneous conditions.

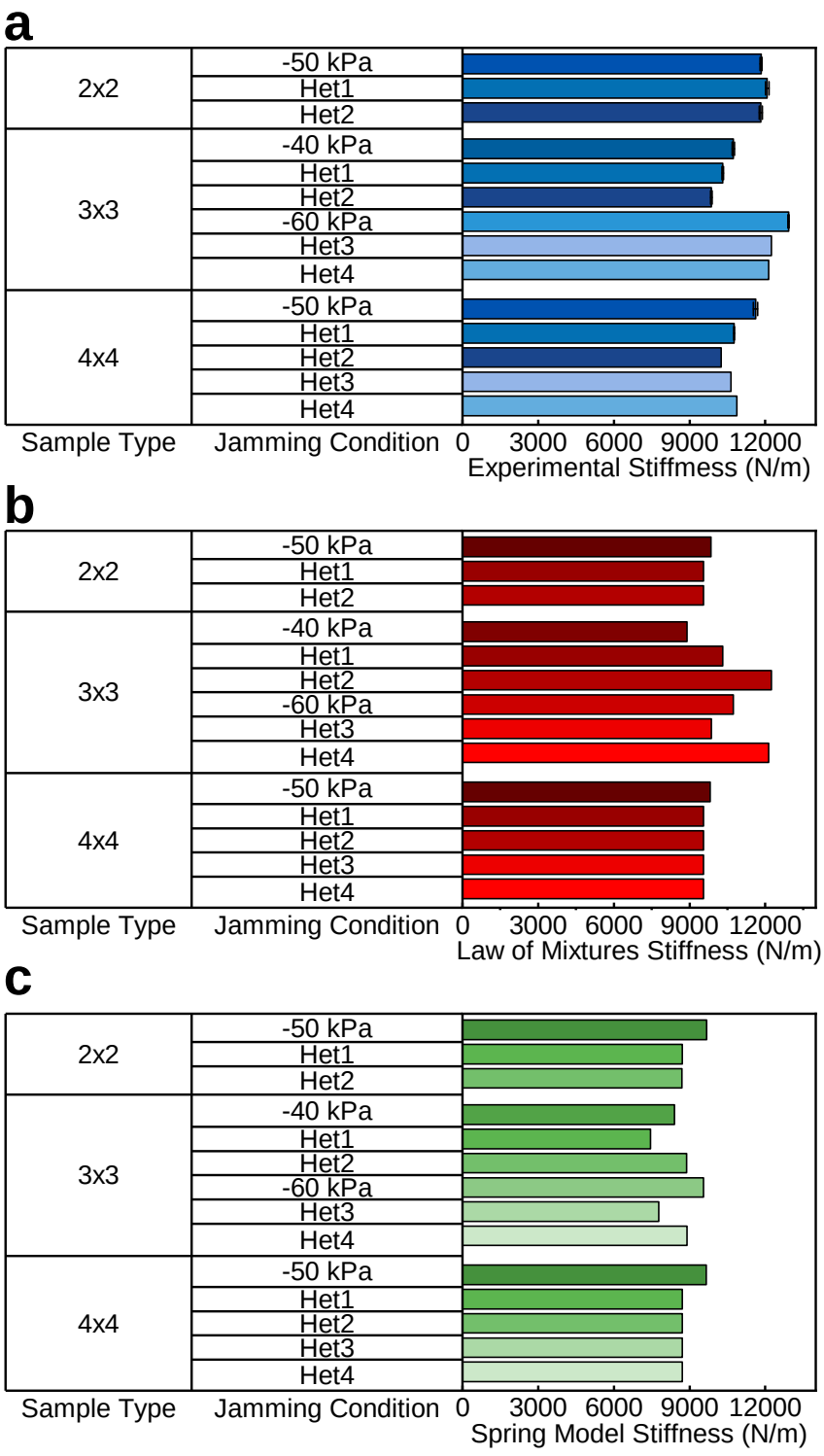

Figure 3.12: **Homogeneous and Heterogeneous Jamming Stiffness Comparison. a)** Experimental Stiffness Comparison. **b)** Law of Mixtures Stiffness Comparison. **c)** Spring System Stiffness Comparison.

Fig. 3.12a displays the experimental stiffness for each homogeneously and heterogeneously jammed condition. For the 2x2 sample, the percentage difference between the homogeneous and heterogeneous configurations is within 2% according to Table A.10, indicating that near equal stiffness can be achieved by either homogeneously or heterogeneously jamming a sample, as long as the average pressure in both conditions is equal. This can also be seen for the 3x3 sample jamming conditions, where Het1 and Het2 have differ from -40 kPa by 3.90% and 8.09% respectively, and Het3 and Het4 differ from -60 kPa by 5.24% and 6.07% respectively. The 4x4 sample also follows a similar pattern, however, with a larger deviation from the homogeneous result. This deviation can be attributed to unpredictable granular behavior within each chamber and varying non-linear interactions between the granular rows and the EcoFlex regions in between.

Sub-figure b in Fig. 3.12 shows the stiffness predictions according to the Law of Mixtures model. Notably, this model seems to underestimate stiffness across most jamming conditions and configurations when compared to the experimental data. For the 2x2 sample under conditions Het1 and Het2, the percentage differences were 2.99% and 3.037% respectively. These deviations highlight the Law of Mixture's ability in accurately predicting the stiffness when the sample has a small matrix, is heterogeneously jammed and therefore, exhibits distinct stiffness. This is a clear indication of oversimplification in the model's handling of localized stiffness changes due to heterogeneous pressure distribution. As for the 3x3 sample, the variance is more prelavent. For Het1, there is a significant overestimation of stiffness with a 15.9% difference, yet for Het2 the difference is much larger at 37.6% according to Table A.11. However, this is not consistent as Het3 and Het4 had smaller deviations at 8.1% and 13.1%. This inconsistency reflects the model's limitation in adjusting with the complexity of the sample matrices. For the 4x4 samples, the percentage differences for Het1 to Het4 ranged from 2.6% to 2.7%, indicating consistency in its stiffness predictions. Overall, this

suggests that the Law of Mixtures model is consistent in its stiffness predictions despite its tendency to underestimate the experimental stiffness.

For the 2x2 sample conditions Het1 and Het2, the Spring System model displays variations ranging between 9.92% and 10.13%. Despite these deviations being larger than that of the Law of Mixtures model, they are more consistent in their approach. Due to the spring assumption, the model incorporates interactions between granular chambers and the surrounding EcoFlex more accurately than the Law of Mixtures model. The 3x3 sample's Het1 and Het2 conditions present a wider range of percent differences, with Het1 at 11.3% and Het2 at 5.7% according to Table A.12, with a similar pattern for Het3 and Het4. For the 4x4 configurations, the results are consistently in the 9% range, similar to the 2x2 sample. This indicates that despite the increases complexity of a larger matrix, the Spring System model maintains a consistent performance.

Overall, the Law of Mixtures model's inconsistent estimation across all jamming configurations (homogeneous, selective, and heterogeneous) point to significant oversimplifications in how it accounts for interactions between different components of the granular composite. It might not fully capture the impact of heterogeneous jamming, where different pressures and densities across the sample could significantly influence the overall stiffness. However, across all configurations, the Spring System model exhibits a consistent alignment with the experimental data, suggesting it may incorporate aspects of the sample's mechanical behavior more effectively than the Law of Mixtures model.

3.5 Conclusion

Under homogeneous jamming conditions, where uniform pressure was applied throughout the sample matrices, the stiffness consistently increased with the magnitude of negative

pneumatic pressure. This direct relationship showcases the predictable behavior of granular composites when subjected to vacuum pressures [68]. In selective jamming conditions, the material's capability to achieve targeted stiffness alterations within localized regions of the composite material was effectively demonstrated. This is a proof of concept for future granular jamming applications that require nuanced control, and is proof that selectively jammed granular composite materials could maintain differentiated stiffness across its matrix. The complexity of selective jamming was then extended to heterogeneous jamming, where different pressures were applied to different rows of the matrix in the granular composite. The aim of this test was to simulate applications were materials might experience non-uniform stress distributions. Notably, the stiffness varied depending on the pressure gradients applied and the matrix type, but the overall stiffness of a heterogeneously jammed sample was nearly equal to that of a homogeneously jammed sample at the same average pressure, despite differing stiffness gradients. These tests underline the adaptability of granular composite materials, further demonstrating their potential in soft robotics. The broad range of stiffness modulation highlights the capability of these materials to meet various demands, especially with the ability to control stiffness at specific locations within a material.

Additionally, I have examined the efficacy of granular jamming for tuning stiffness in soft robotics, employing the Law of Mixtures and Spring System models. The analysis highlights the strengths and limitations in accurately predicting the stiffness of granular composite materials under varied experimental conditions. The findings reveal that while both models underestimate stiffness for different jamming conditions, the Spring System model aligns more consistently with experimental data across different jamming scenarios. The success of this model is due to assuming elastic behavior for the granular media interactions, which is more reflective of the observed experimental behaviors. In contrast, the Law of Mixtures fails to account for the complexities of selective jamming, leading to significant discrepancies

in stiffness predictions.

In conclusion, the comprehensive analysis of granular jamming techniques through this research provides insights into the current capabilities and limitations of stiffness tuning in soft robotics.

Chapter 4

Conclusions

4.1 Granular Composite with Adjustable and Tunable Stiffness

In summary, this thesis presents a granular composite material with rapid adjustable and tunable stiffness. The material stiffness is modulated via a customized pneumatic system that takes advantage of the granular media inside of the material via granular jamming. This approach allows for a material to have varying stiffness fields while being reversible and tunable. The stiffness models developed here present a framework for future stiffness tuning applications for granular jamming applications requiring stiffness tuning.

4.2 Contributions

- Developed custom pneumatics for granular jamming applications. The development of the custom pneumatic system in Fig. 3.3.2 enhances the experimental capabilities of granular jamming applications, as it allows for precise control over the application of negative pressure into the granular composite while integrating pressure sensors, regulators, valves, and a digital acquisition system to ensure accurate, reproducible jamming. The ability to independently control pressure in each row is critical for exploring the effects of selective and

heterogeneous jamming. This system can be adapted for use in different scenarios encountered in soft robotics.

- Experimental validation of stiffness tunability. Testing was conducted to validate the relationship between vacuum pressure and the resulting stiffness changes. These tests covered different jamming conditions, providing a robust dataset that confirms the tunable nature of the granular composite material.

- Predictive modeling of granular composites. The thesis introduces two predictive models, the first is adapted from the Law of Mixtures and the second assumes a one dimensional spring system to estimate the stiffness of granular composite materials under varying jamming conditions.

- Detailed analysis of jamming mechanisms. The thesis provides an in-depth examination of how different jamming configurations affect the mechanical properties of the composite material. This analysis is pivotal for understanding the mechanisms that govern the transition between unjammed and jammed states for stiffness tuning.

4.3 Future Work

Future investigations of this thesis should be focused on the following.

- Advancements in pneumatic systems for stiffness modulation. This would include a more advanced pressure regulator to ensure a higher degree of control on negative pressure. This could also be integrated with more advanced negative pressure sensors that can produce more accurate readings and real-time feedback. Finally, another addition would be the implementation of digitally controlled, vacuum proof two way, two position solenoid valves to allow for more control over the jamming states of the granular composite.

- Predictive modeling of granular composites. A staged viscoelastic rheological model can be developed for stiffness prediction. This model can be used to predict the material's response over time while experiencing creep or relaxation, and can account for non-linear behavior. From there, finite element analysis can be potentially used to develop a new predictive model for the granular composites that can account for the non-linear behavior of granular media, in addition to its interactions with EcoFlex. The finite element analysis can also be used to further investigate the micro-scale interactions within the granular media.

- Application-specific design. This granular composite material can be adapted for specific applications such as wearable exoskeletons and shock absorbers in robotic limbs.

Bibliography

[1] *Granular Jamming With Hydraulic Control*, volume 6A: 37th Mechanisms and Robotics Conference of *International Design Engineering Technical Conferences and Computers and Information in Engineering Conference*, 2013.

[2] Loai Al Abeach, Samia Nefti-Meziani, Theo Theodoridis, and Steve Davis. A variable stiffness soft gripper using granular jamming and biologically inspired pneumatic muscles. *Journal of Bionic Engineering*, 15:236–246, 2018.

[3] John Amend, Nadia Cheng, Sami Fakhouri, and Bill Culley. Soft robotics commercialization: Jamming grippers from research to product. *Soft robotics*, 3(4):213–222, 2016.

[4] Katalin Bagi. On the concept of jammed configurations from a structural mechanics perspective. *Granular Matter*, 9(1):109–134, 2007.

[5] Silvestro Barbarino, Onur Bilgen, Rafic M Ajaj, Michael I Friswell, and Daniel J Inman. A review of morphing aircraft. *Journal of intelligent material systems and structures*, 22(9):823–877, 2011.

[6] Silvestro Barbarino, EI Saavedra Flores, Rafic M Ajaj, Iman Dayyani, and Michael I Friswell. A review on shape memory alloys with applications to morphing aircraft. *Smart materials and structures*, 23(6):063001, 2014.

[7] Edward J Barron III, Ella T Williams, Ravi Tutika, Nathan Lazarus, and Michael D Bartlett. A unified understanding of magnetorheological elastomers for rapid and extreme stiffness tuning. *RSC Applied Polymers*, 2023.

[8] Michael D Bartlett, Eric J Markvicka, and Carmel Majidi. Rapid fabrication of soft, multilayered electronics for wearable biomonitoring. *Advanced Functional Materials*, 26 (46):8496–8504, 2016.

[9] Robert P Behringer. Jamming in granular materials. *Comptes Rendus. Physique*, 16 (1):10–25, 2015.

[10] Philip R Bevington and D Keith Robinson. Data reduction and error analysis. *McGraw Hill, New York*, 2003.

[11] Shantonu Biswas and Yon Visell. Emerging material technologies for haptics. *Advanced Materials Technologies*, 4(4):1900042, 2019.

[12] Nabil Bouhfid, Marya Raji, Radouane Boujmal, Hamid Essabir, Mohammed-Ouadi Bensalah, Rachid Bouhfid, and Abou el kacem Qaiss. 5 - numerical modeling of hybrid composite materials. In Mohammad Jawaid, Mohamed Thariq, and Naheed Saba, editors, *Modelling of Damage Processes in Biocomposites, Fibre-Reinforced Composites and Hybrid Composites*, Woodhead Publishing Series in Composites Science and Engineering, pages 57–101. Woodhead Publishing, 2019. ISBN 978-0-08-102289-4. doi: https://doi.org/10.1016/B978-0-08-102289-4.00005-9. URL https://www.sciencedirect.com/science/article/pii/B9780081022894000059.

[13] J David Brigido-González, Steve G Burrow, and Benjamin KS Woods. Switchable stiffness morphing aerostructures based on granular jamming. *Journal of Intelligent Material Systems and Structures*, 30(17):2581–2594, 2019.

[14] Eric Brown, Nicholas Rodenberg, John Amend, Annan Mozeika, Erik Steltz, Mitchell R Zakin, Hod Lipson, and Heinrich M Jaeger. Universal robotic gripper based on the jamming of granular material. *Proceedings of the National Academy of Sciences*, 107 (44):18809–18814, 2010.

[15] Charles S Campbell. Granular material flows–an overview. *Powder Technology*, 162(3): 208–229, 2006.

[16] ME Cates, JP Wittmer, J-P Bouchaud, and Ph Claudin. Jamming, force chains, and fragile matter. *Physical review letters*, 81(9):1841, 1998.

[17] Bulbul Chakraborty and Bob Behringer. Jamming of granular matter. In *Statistical and Nonlinear Physics*, pages 397–426. Springer, 2022.

[18] Boyce S Chang, Ravi Tutika, Joel Cutinho, Stephanie Oyola-Reynoso, Jiahao Chen, Michael D Bartlett, and Martin M Thuo. Mechanically triggered composite stiffness tuning through thermodynamic relaxation (st3r). *Materials Horizons*, 5(3):416–422, 2018.

[19] Ragesh Chellattoan and Gilles Lubineau. A stretchable fiber with tunable stiffness for programmable shape change of soft robots. 11 2021.

[20] Nadia Cheng, John Amend, Todd Farrell, Debra Latour, Carlos Martinez, Jen Johansson, Anthony McNicoll, Marek Wartenberg, Samuel Naseef, William Hanson, et al. Prosthetic jamming terminal device: A case study of untethered soft robotics. *Soft robotics*, 3(4):205–212, 2016.

[21] Nadia G Cheng, Maxim B Lobovsky, Steven J Keating, Adam M Setapen, Katy I Gero, Anette E Hosoi, and Karl D Iagnemma. Design and analysis of a robust, low-cost, highly articulated manipulator enabled by jamming of granular media. In *2012 IEEE international conference on robotics and automation*, pages 4328–4333. IEEE, 2012.

[22] Jasper Delaey, Peter Dubruel, and Sandra Van Vlierberghe. Shape-memory polymers for biomedical applications. *Advanced Functional Materials*, 30(44):1909047, 2020.

[23] David A Dillard, Bikramjit Mukherjee, Preetika Karnal, Romesh C Batra, and Joelle Frechette. A review of winkler's foundation and its profound influence on adhesion and soft matter applications. *Soft matter*, 14(19):3669–3683, 2018.

[24] Walter Federle and David Labonte. Dynamic biological adhesion: mechanisms for controlling attachment during locomotion. *Philosophical Transactions of the Royal Society B*, 374(1784):20190199, 2019.

[25] Seth G. Fitzgerald, Gary W. Delaney, and David Howard. A review of jamming actuation in soft robotics. *Actuators*, 9(4), 2020. ISSN 2076-0825. doi: 10.3390/act9040104. URL https://www.mdpi.com/2076-0825/9/4/104.

[26] Seth G Fitzgerald, Gary W Delaney, and David Howard. A review of jamming actuation in soft robotics. In *Actuators*, volume 9, page 104. MDPI, 2020.

[27] Sean T Frey, ABM Tahidul Haque, Ravi Tutika, Elizabeth V Krotz, Chanhong Lee, Cole B Haverkamp, Eric J Markvicka, and Michael D Bartlett. Octopus-inspired adhesive skins for intelligent and rapidly switchable underwater adhesion. *Science Advances*, 8(28):eabq1905, 2022.

[28] J Gilbert, M Patton, C Mullen, and S Black. Vacuumatics, 4th year research project. *Department of Architecture and Planning, Queen's University, Belfast*, 1970.

[29] Yangtai Hao, Jianye Gao, Yonggang Lv, and Jing Liu. Low melting point alloys enabled stiffness tunable advanced materials. *Advanced Functional Materials*, 32(25):2201942, 2022.

[30] Cole B Haverkamp, Dohgyu Hwang, Chanhong Lee, and Michael D Bartlett. Deterministic control of adhesive crack propagation through jamming based switchable adhesives. *Soft Matter*, 17(7):1731–1737, 2021.

[31] David Howard, Jack O'Connor, Jordan Letchford, Therese Joseph, Sophia Lin, Sarah Baldwin, and Gary Delaney. A comprehensive dataset of grains for granular jamming in soft robotics: Grip strength and shock absorption. In *2023 IEEE International Conference on Soft Robotics (RoboSoft)*, pages 1–8. IEEE, 2023.

[32] K Iwashita and Masaya Oda. *Mechanics of granular materials: an introduction*. CRC press, 2020.

[33] Heinrich M Jaeger, Sidney R Nagel, and Robert P Behringer. The physics of granular materials. *Physics today*, 49(4):32–38, 1996.

[34] Robert M Jones. *Mechanics of composite materials*. CRC press, 2018.

[35] Christophe Josserand, Alexei V Tkachenko, Daniel M Mueth, and Heinrich M Jaeger. Memory effects in granular materials. *Physical review letters*, 85(17):3632, 2000.

[36] Deok-Ho Kim, Moon Gu Lee, Byungkyu Kim, and Yu Sun. A superelastic alloy microgripper with embedded electromagnetic actuators and piezoelectric force sensors: a numerical and experimental study. *Smart materials and structures*, 14(6):1265, 2005.

[37] Anthony J Kinloch. *Adhesion and adhesives: science and technology*. Springer Science & Business Media, 2012.

[38] Chandan Kumar, Adam Redman, William Leggate, Robert L McGavin, and Tony Dakin. Assessment of the application of a smart thumper™ as a low-cost and portable device used for stiffness estimation of timber products. *BioResources*, 16(3):5838, 2021.

[39] Nishant Kumar and Stefan Luding. Memory of jamming–multiscale models for soft and granular matter. *Granular Matter*, 18(3):58, 2016.

[40] Junghan Kwon, Inrak Choi, Myungsun Park, Jeongin Moon, Bomin Jeong, Prabhat Pathak, Jooeun Ahn, and Yong-Lae Park. Selectively stiffening garments enabled by cellular composites. *Advanced Materials Technologies*, 7(9):2101543, 2022.

[41] Cecilia Laschi, Barbara Mazzolai, and Matteo Cianchetti. Soft robotics: Technologies and systems pushing the boundaries of robot abilities. *Science Robotics*, 1(1):eaah3690, 2016.

[42] Chanhong Lee, Huiqi Shi, Jiyoung Jung, Bowen Zheng, Kan Wang, Ravi Tutika, Rong Long, Bruce P Lee, Grace X Gu, and Michael D Bartlett. Bioinspired materials for underwater adhesion with pathways to switchability. *Cell Reports Physical Science*, 4 (10), 2023.

[43] Jinsong Leng, Xin Lan, Yanju Liu, and Shanyi Du. Shape-memory polymers and their composites: stimulus methods and applications. *Progress in Materials Science*, 56(7): 1077–1135, 2011.

[44] Vrad Levering, Qiming Wang, Phanindhar Shivapooja, Xuanhe Zhao, and Gabriel P López. Soft robotic concepts in catheter design: an on-demand fouling-release urinary catheter. *Advanced healthcare materials*, 3(10):1588–1596, 2014.

[45] Stephen Licht, Everett Collins, Manuel Lopes Mendes, and Christopher Baxter. Stronger at depth: Jamming grippers as deep sea sampling tools. *Soft robotics*, 4 (4):305–316, 2017.

[46] Andrea J Liu and Sidney R Nagel. Jamming is not just cool any more. *Nature*, 396 (6706):21–22, 1998.

[47] Andrea J Liu and Sidney R Nagel. *Jamming and rheology: constrained dynamics on microscopic and macroscopic scales*. CRC Press, 2001.

[48] Ziyang Liu and Feng Yan. Switchable adhesion: on-demand bonding and debonding. *Advanced Science*, 9(12):2200264, 2022.

[49] Shaunak A Mehta, Yeunhee Kim, Joshua Hoegerman, Michael D Bartlett, and Dylan P Losey. Riso: Combining rigid grippers with soft switchable adhesives. In *2023 IEEE International Conference on Soft Robotics (RoboSoft)*, pages 1–8. IEEE, 2023.

[50] Harper Meng and Guoqiang Li. A review of stimuli-responsive shape memory polymer composites. *polymer*, 54(9):2199–2221, 2013.

[51] Amir Mohammadi Nasab, Siavash Sharifi, Shuai Chen, Yang Jiao, and Wanliang Shan. Robust three-component elastomer–particle–fiber composites with tunable properties for soft robotics. *Advanced Intelligent Systems*, 3(2):2000166, 2021.

[52] D Moorhouse, B Sanders, M Von Spakovsky, and J Butt. Benefits and design challenges of adaptive structures for morphing aircraft. *The Aeronautical Journal*, 110(1105): 157–162, 2006.

[53] Bobak Mosadegh, Panagiotis Polygerinos, Christoph Keplinger, Sophia Wennstedt, Robert F. Shepherd, Unmukt Gupta, Jongmin Shim, Katia Bertoldi, Conor J. Walsh, and George M. Whitesides. Pneumatic networks for soft robotics that actuate rapidly. *Advanced Functional Materials*, 24(15):2163–2170, 2014. doi: https://doi.org/10.1002/adfm.201303288. URL https://onlinelibrary.wiley.com/doi/abs/10.1002/adfm.201303288.

[54] Jong-Seok Oh and Seung-Bok Choi. State of the art of medical devices featuring smart electro-rheological and magneto-rheological fluids. *Journal of King Saud University - Science*, 29(4):390–400, 2017. ISSN 1018-3647. doi: https://doi.org/10.1016/j.jksus.2017.05.012. URL https://www.sciencedirect.com/science/article/pii/S1018364717302616. SI: Smart materials applications of new materials.

[55] ASTM Committee D11 on Rubber and Rubber like Materials. Subcommittee D11. 10 on Physical Testing. *Standard test methods for rubber properties in compression*. ASTM International, 2018.

[56] Gianluca Palli. Model and control of tendon actuated robots. 2007.

[57] Yu-Jin Park and Seung-Bok Choi. Sensors and sensing devices utilizing electrorheological fluids and magnetorheological materials—a review. *Sensors*, 24(9):2842, 2024.

[58] Dan Peretz and AT DiBenedetto. Crack propagation in polymeric composites. *Engineering fracture mechanics*, 4(4):979–990, 1972.

[59] Lorenza Petrini and Francesco Migliavacca. Biomedical applications of shape memory alloys. *Journal of Metallurgy*, 2011(1):501483, 2011.

[60] Sebastian Reitelshöfer, Christina Ramer, Daniel Gräf, Falko Matern, and Jörg Franke. Combining a collaborative robot and a lightweight jamming-gripper to realize an intuitively to use and flexible co-worker. In *2014 IEEE/SICE International Symposium on System Integration*, pages 1–5. IEEE, 2014.

[61] Junius Santoso, Erik H Skorina, Marco Salerno, Sébastien de Rivaz, Jamie Paik, and Cagdas D Onal. Single chamber multiple degree-of-freedom soft pneumatic actuator enabled by adjustable stiffness layers. *Smart Materials and Structures*, 28(3):035012, 2019.

[62] Jun Shintake, Vito Cacucciolo, Dario Floreano, and Herbert Shea. Soft robotic grippers. *Advanced materials*, 30(29):1707035, 2018.

[63] Bruno Siciliano, Oussama Khatib, and Torsten Kröger. *Springer handbook of robotics*, volume 200. Springer, 2008.

[64] Kunal Singh and Shilpa Gupta. Controlled actuation, adhesion, and stiffness in soft robots: A review. *Journal of Intelligent & Robotic Systems*, 106(3):59, 2022.

[65] Sukho Song, Dirk-Michael Drotlef, Carmel Majidi, and Metin Sitti. Controllable load sharing for soft adhesive interfaces on three-dimensional surfaces. *Proceedings of the National Academy of Sciences*, 114(22):E4344–E4353, 2017.

[66] M. Sreelakshmi and T.D. Subash. Haptic technology: A comprehensive review on its applications and future prospects. *Materials Today: Proceedings*, 4(2, Part B): 4182–4187, 2017. ISSN 2214-7853. doi: https://doi.org/10.1016/j.matpr.2017.02.120. URL https://www.sciencedirect.com/science/article/pii/S2214785317303188. International Conference on Computing, Communication, Nanophotonics, Nanoscience, Nanomaterials and Nanotechnology.

[67] Andrew A. Stanley. *Haptic Jamming: Controllable Mechanical Properties in a Shape-Changing User Interface*. PhD thesis, 2016. URL http://login.ezproxy.lib.vt.edu/login?url=https://www.proquest.com/dissertations-theses/haptic-jamming-controllable-mechanical-properties/docview/2451129676/se-2. Copyright - Database copyright ProQuest LLC; ProQuest does not claim copyright in the individual underlying works; Last updated - 2024-03-20.

[68] Andrew A Stanley and Allison M Okamura. Controllable surface haptics via particle jamming and pneumatics. *IEEE transactions on haptics*, 8(1):20–30, 2015.

[69] Andrew A Stanley, James C Gwilliam, TN Judkins, and AM Okamura. A haptic display for medical simulation using particle jamming. In *Proc. Medicine Meets Virtual Reality*, volume 20, 2013.

[70] Andrew A Stanley, James C Gwilliam, and Allison M Okamura. Haptic jamming: A

deformable geometry, variable stiffness tactile display using pneumatics and particle jamming. In *2013 World Haptics Conference (WHC)*, pages 25–30. IEEE, 2013.

[71] RSJL Stanway, JL Sproston, and AK El-Wahed. Applications of electro-rheological fluids in vibration control: a survey. *Smart Materials and Structures*, 5(4):464, 1996.

[72] Jian Sun, Qinghua Guan, Yanju Liu, and Jinsong Leng. Morphing aircraft based on smart materials and structures: A state-of-the-art review. *Journal of Intelligent material systems and structures*, 27(17):2289–2312, 2016.

[73] Igor Svetel. Prof. ivan petrovic, phd, m. arch (1932-2000). *Automation in Construction*, 11(2):129–130, 2002.

[74] Charnwit Tridech, Henry A Maples, Paul Robinson, and Alexander Bismarck. High performance composites with active stiffness control. *ACS applied materials & interfaces*, 5(18):9111–9119, 2013.

[75] Nicholas W Tschoegl. *The phenomenological theory of linear viscoelastic behavior: an introduction*. Springer Science & Business Media, 2012.

[76] Valentina Vitiello, Su-Lin Lee, Thomas P Cundy, and Guang-Zhong Yang. Emerging robotic platforms for minimally invasive surgery. *IEEE reviews in biomedical engineering*, 6:111–126, 2012.

[77] Susan Watkins and Lucy Dunne. *Functional clothing design: From sportswear to spacesuits*. Bloomsbury Publishing USA, 2015.

[78] Michael Wehner, Brendan Quinlivan, Patrick M Aubin, Ernesto Martinez-Villalpando, Michael Baumann, Leia Stirling, Kenneth Holt, Robert Wood, and Conor Walsh. A lightweight soft exosuit for gait assistance. In *2013 IEEE international conference on robotics and automation*, pages 3362–3369. IEEE, 2013.

[79] Sebastian Wolf, Giorgio Grioli, Oliver Eiberger, Werner Friedl, Markus Grebenstein, Hannes Höppner, Etienne Burdet, Darwin G Caldwell, Raffaella Carloni, Manuel G Catalano, et al. Variable stiffness actuators: Review on design and components. *IEEE/ASME transactions on mechatronics*, 21(5):2418–2430, 2015.

[80] Benjamin K Woods and Michael I Friswell. Structural characterization of the fish bone active camber morphing airfoil. In *22nd AIAA/ASME/AHS adaptive structures conference*, page 1122, 2014.

[81] Yuliang Xia, Yang He, Fenghua Zhang, Yanju Liu, and Jinsong Leng. A review of shape memory polymers and composites: mechanisms, materials, and applications. *Advanced materials*, 33(6):2000713, 2021.

[82] Hongbo Zeng, Yu Wang, Tao Jiang, Hongqin Xia, Xue Gu, and Hongxu Chen. Recent progress of biomimetic motions—from microscopic micro/nanomotors to macroscopic actuators and soft robotics. *RSC advances*, 11(44):27406–27419, 2021.

Appendices

Appendix A

Appendix

A.1 Experimental and Model Stiffness Comparison Tables

The following tables contain the experimental, Law of Mixtures, and Spring System stiffness for each jamming condition, as plotted in Figures **??**. **??**, and **??**.

Here are the tables for Homogenenous Jamming:

Table A.1: Homogeneous Stiffness Comparison for 2x2 Sample

Pressure (kPa)	Experimental Stiffness (N/m)	Standard Deviation (N/m)	Law of Mixtures Stiffness (N/m)	Spring Stiffness (N/m)
0	1765.5	10.8	3198.7	2074.6
-10	5416.0	50.1	5446.2	5721.5
-20	7773.1	37.6	6759.3	7209.7
-30	9172.7	47.7	7893.0	8251.7
-40	10 803.9	37.9	8892.4	9029.7
-50	11 831.6	41.0	9848.9	9676.6
-60	12 665.2	35.3	10 720.9	10 197.9
-70	13 528.9	75.6	11 576.2	10 656.2
-80	13 925.9	60.5	12 355.3	11 034.4

Table A.2: Homogeneous Stiffness Comparison for 3x3 Sample

Pressure (kPa)	Experimental Stiffness (N/m)	Standard Deviation (N/m)	Law of Mixtures Stiffness (N/m)	Spring System Stiffness (N/m)
0	2144.2	14.9	3238.5	2090.9
-10	5688.6	38.4	5453.6	5290.8
-20	7820.8	40.3	6754.9	6658.5
-30	9041.3	39.7	7870.6	7631.7
-40	10 729.5	44.3	8896.8	8401.3
-50	12 055.5	32.1	9841.9	9023.9
-60	12 920.8	24.5	10 732.9	9547.9
-70	13 771.8	21.9	11 586.7	10 001.4
-80	14 067.6	20.5	12 358.1	10 375.6

Table A.3: Homogeneous Stiffness Comparison for 4x4 Sample

Pressure (kPa)	Experimental Stiffness (N/m)	Standard Deviation (N/m)	Law of Mixtures Stiffness (N/m)	Spring Stiffness (N/m)
0	2323.4	10.7	3318.2	2317.8
-10	5221.4	34.9	5379.8	5636.2
-20	7553.8	52.4	6706.2	7155.9
-30	9542.9	51.5	7855.6	8220.1
-40	10 407.1	77.6	8879.1	9019.9
-50	11 614.4	89.3	9818.7	9657.3
-60	12 740.0	45.5	10 713.5	10 193.5
-70	13 193.2	55.5	11 552.3	10 643.8
-80	13 843.3	36.6	12 354.2	11 033.7

Here are the tables for Selective Jamming:

Table A.4: Selective Stiffness Comparison for 2x2 Sample

Selected Row	Experimental Stiffness (N/m)	Standard Deviation (N/m)	Law of Mixtures Stiffness (N/m)	Spring Stiffness (N/m)
Row 1	3716.3	44.1	7791.0	3486.3
Row 2	3791.1	43.4	7817.7	3691.9

Table A.5: Selective Stiffness Comparison for 3x3 Sample

Selected Row	Experimental Stiffness (N/m)	Standard Deviation (N/m)	Law of Mixtures Stiffness (N/m)	Spring Stiffness (N/m)
Row 1	3316.9	27.1	6282.6	2798.1
Row 2	3564.1	34.4	6312.7	2910.1
Row 3	3164.9	26.7	6274.1	2853.6

Table A.6: Selective Stiffness Comparison for 4x4 Sample

Selected Row	Experimental Stiffness (N/m)	Standard Deviation (N/m)	Law of Mixtures Stiffness (N/m)	Spring Stiffness (N/m)
Row 1	3581.3	26.5	5501.9	2633.0
Row 2	4188.1	37.2	5513.5	2684.9
Row 3	3958.7	34.9	5494.5	2599.1
Row 4	3234.9	23.4	5507.9	2668.2

Here are the tables for Heterogeneous Jamming:

Table A.7: Heterogeneous Stiffness Comparison for 2x2 Sample

Heterogeneous Jamming Condition	Experimental Stiffness (N/m)	Standard Deviation (N/m)	Law of Mixtures Stiffness (N/m)	Spring Stiffness (N/m)
Het1	12 078.8	77.5	9554.4	8716.1
Het2	11 821.1	66.8	9549.8	8696.6

Table A.8: Heterogeneous Stiffness Comparison for 3x3 Sample

Heterogeneous Jamming Condition	Experimental Stiffness (N/m)	Standard Deviation (N/m)	Law of Mixtures Stiffness (N/m)	Spring Stiffness (N/m)
Het1	10 311.3	32.2	8621.0	7453.9
Het2	9861.1	27.1	8617.4	7770.7
Het3	12 243.4	25.9	10 492.4	8881.5
Het4	12 136.4	26.2	10 495.9	8895.5

Table A.9: Heterogeneous Stiffness Comparison for 4x4 Sample

Heterogeneous Jamming Condition	Experimental Stiffness (N/m)	Standard Deviation (N/m)	Law of Mixtures Stiffness (N/m)	Spring Stiffness (N/m)
Het1	10 762.8	19.4	9555.2	8716.5
Het2	10 244.6	24.3	9552.7	8707.0
Het3	10 637.3	37.6	9552.5	8706.3
Het4	10 873.1	42.5	9552.6	8706.6

A.2 Homogeneous and Heterogeneous Stiffness Comparison Tables

The following tables contain the stiffness and percentage difference data for the homogeneous and heterogeneous stiffness data plotted in Fig. 3.12.

Table A.10: Experimental Homogeneous and Heterogeneous Jamming Stiffness

Sample Matrix Type	Homogeneous Pressure (kPa)	Stiffness (N/m)	Heterogeneous Condition	Stiffness (N/m)	Percent Difference (%)
2x2	−50.0	11 831.6	Het1	12 078.0	2.1
2x2	−50.0	11 831.6	Het2	11 821.1	0.1
3x3	−40.0	10 729.5	Het1	10 311.3	3.9
3x3	−40.0	10 729.5	Het2	9861.3	8.1
3x3	−60.0	12 920.8	Het3	12 243.4	5.2
3x3	−60.0	12 920.8	Het4	12 136.4	6.1
4x4	−50.0	11 614.4	Het1	10 762.8	7.3
4x4	−50.0	11 614.4	Het2	10 244.6	11.8
4x4	−50.0	11 614.4	Het3	10 637.3	8.4
4x4	−50.0	11 614.4	Het4	10 873.1	6.4

Table A.11: Law of Mixtures Homogeneous and Heterogeneous Jamming Stiffness

Sample Matrix Type	Homogeneous Pressure (kPa)	Stiffness (N/m)	Heterogeneous Condition	Stiffness (N/m)	Percent Difference (%)
2x2	−50.0	9848.9	Het1	9554.4	3.0
2x2	−50.0	9848.9	Het2	9549.8	3.0
3x3	−40.0	8896.8	Het1	10 311.3	15.9
3x3	−40.0	8896.8	Het2	12 243.4	37.6
3x3	−60.0	10 732.9	Het3	9861.1	8.1
3x3	−60.0	10 732.9	Het4	12 136.4	13.1
4x4	−50.0	9818.7	Het1	9555.2	2.7
4x4	−50.0	9818.7	Het2	9552.7	2.7
4x4	−50.0	9818.7	Het3	9552.5	2.7
4x4	−50.0	9818.7	Het4	9552.6	2.7

Table A.12: Spring System Homogeneous and Heterogeneous Jamming Stiffness

Sample Matrix Type	Homogeneous Pressure (kPa)	Stiffness (N/m)	Heterogeneous Condition	Stiffness (N/m)	Percent Difference (%)
2x2	−50.0	9676.6	Het1	8716.1	9.9
2x2	−50.0	9676.6	Het2	8696.6	10.1
3x3	−40.0	8401.3	Het1	7453.9	11.3
3x3	−40.0	8401.3	Het2	8881.5	5.7
3x3	−60.0	9547.9	Het3	7770.7	18.6
3x3	−60.0	9547.9	Het4	8895.5	6.8
4x4	−50.0	9657.3	Het1	8716.5	9.7
4x4	−50.0	9657.3	Het2	8707.0	9.8
4x4	−50.0	9657.3	Het3	8706.3	9.8
4x4	−50.0	9657.3	Het4	8706.6	9.8